



^{18}F -DCFPyL Image Interpretation Training

Andrei Iagaru, MD
Steven Rowe, MD, PhD

- ✓ **Introduction**
- ✓ **Scanning protocols**
- ✓ **^{18}F DCFPyL vs. other PSMA targeting PET radiopharmaceuticals**
- ✓ **Image Interpretation**
- ✓ **Pearls and pitfalls**
- ✓ **Reporting ^{18}F DCFPyL PET**
- ✓ **Image Interpretation Cases**

Case list

Case 1: [Normal biodistribution](#)

Case 2: [Primary staging, high PSA, prostate gland](#)

Case 3: [Post-RP, very low PSA, lymph nodes](#)

Case 4: [Primary staging, prostate](#)

Case 5: [Primary Staging, high PSA, prostate findings](#)

Case 6: [Post-EBRT, subtle lymph nodes](#)

Case 7: [BCR, celiac ganglia](#)

Case 8: [Post-RP and EBRT, inguinal node and urinary issues](#)

Case 9: [Primary staging, rib finding and discussion](#)

Case 10: [Post-RP/PLND/EBRT, lung finding](#)

Case 11: [Post-EBRT, prostate finding](#)

Case 12: [BCR, low PSA skull and lung finding](#)



Case 13: [BCR, testicular finding](#)

Introduction



Society of Nuclear Medicine and Molecular Imaging

Cancer Statistics - 2021

Estimated New Cases

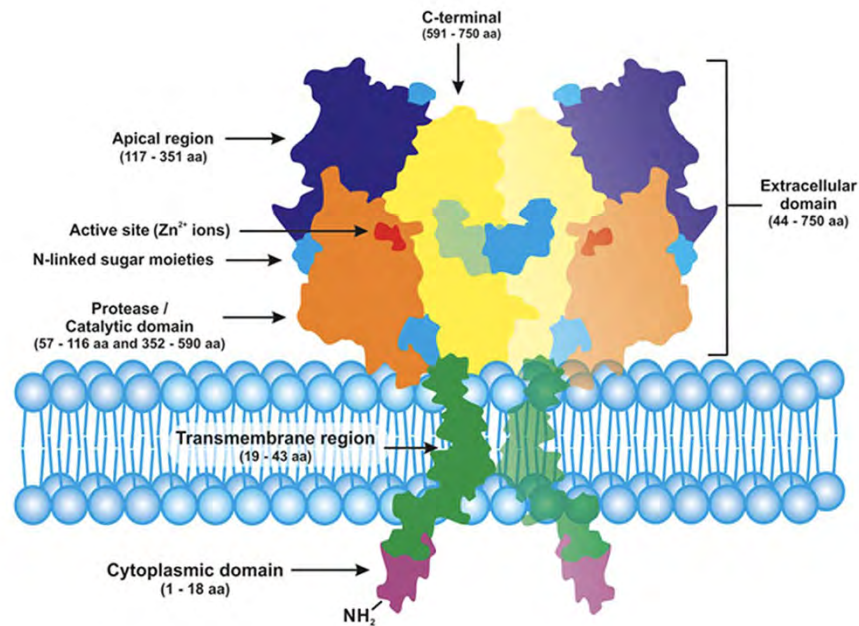
			Males	Females			
Prostate	248,530	26%			Breast	281,550	30%
Lung & bronchus	119,100	12%			Lung & bronchus	116,660	13%
Colon & rectum	79,520	8%			Colon & rectum	69,980	8%
Urinary bladder	64,280	7%			Uterine corpus	66,570	7%
Melanoma of the skin	62,260	6%			Melanoma of the skin	43,850	5%
Kidney & renal pelvis	48,780	5%			Non-Hodgkin lymphoma	35,930	4%
Non-Hodgkin lymphoma	45,630	5%			Thyroid	32,130	3%
Oral cavity & pharynx	38,800	4%			Pancreas	28,480	3%
Leukemia	35,530	4%			Kidney & renal pelvis	27,300	3%
Pancreas	31,950	3%			Leukemia	25,560	3%
All Sites	970,250	100%			All Sites	927,910	100%

Estimated Deaths

			Males	Females			
Lung & bronchus	69,410	22%			Lung & bronchus	62,470	22%
Prostate	34,130	11%			Breast	43,600	15%
Colon & rectum	28,520	9%			Colon & rectum	24,460	8%
Pancreas	25,270	8%			Pancreas	22,950	8%
Liver & intrahepatic bile duct	20,300	6%			Ovary	22,950	5%
Leukemia	13,900	4%			Uterine corpus	12,940	4%
Esophagus	12,410	4%			Liver & intrahepatic bile duct	9,930	3%
Urinary bladder	12,260	4%			Leukemia	9,760	3%
Non-Hodgkin lymphoma	12,170	4%			Non-Hodgkin lymphoma	8,550	3%
Brain & other nervous system	10,500	3%			Brain & other nervous system	8,100	3%
All Sites	319,420	100%			All Sites	289,150	100%

CA Cancer J Clin 2021;71:7-33.

Prostate Specific Membrane Antigen



O'Driscoll et al Br. J. Pharmacol. 2016, 173, 3041.

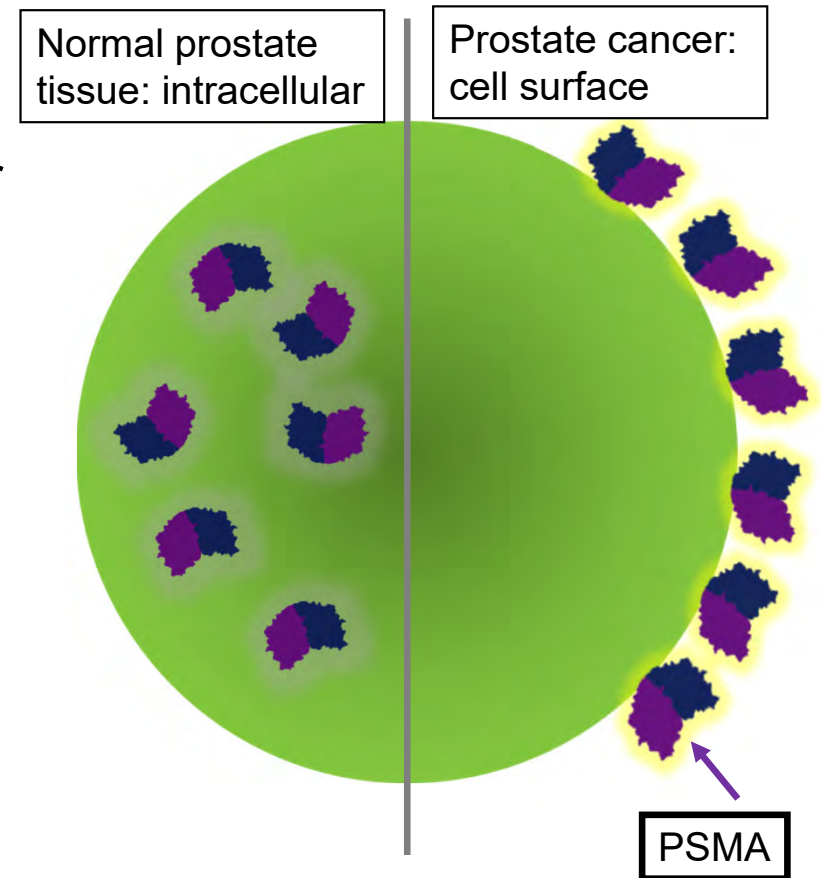
Prostate-specific membrane antigen (PSMA) is a transmembrane protein overexpressed in prostate cancer; PSMA has known enzymatic activities and acts as a glutamate-preferring carboxypeptidase.

Prostate Specific Membrane Antigen (PSMA)

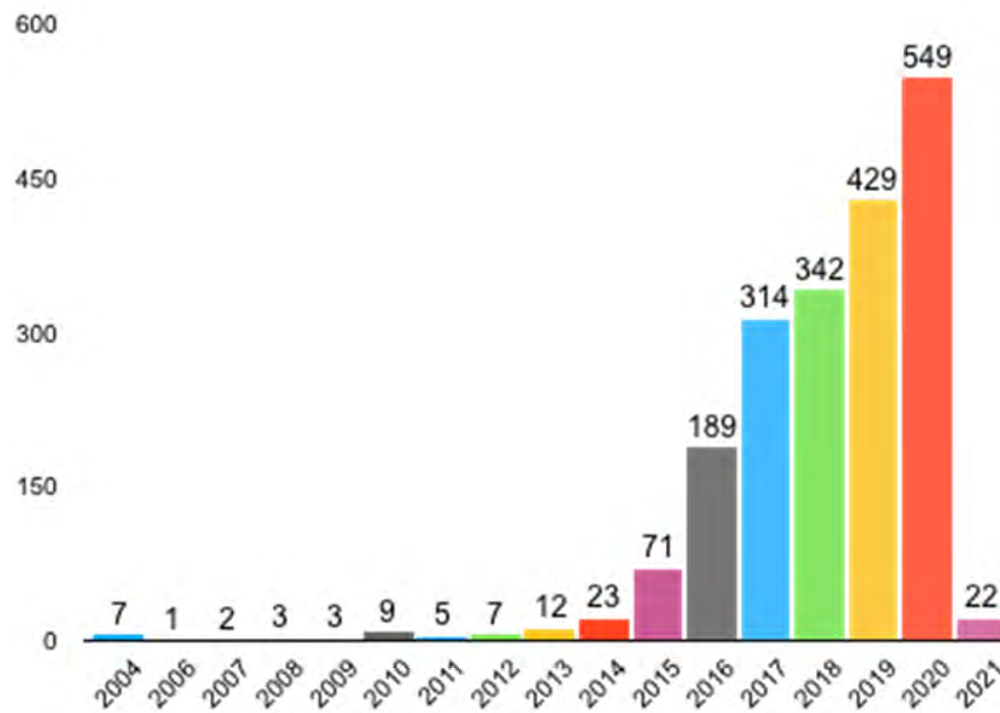
- PSMA expression is primarily extracellular in prostate cancer vs. intracellular in normal prostate tissue
- Expression in normal tissues
 - Prostate epithelium
 - Proximal convoluted renal tubules
 - Jejunal brush border (small intestine)
 - Nervous system ganglia
 - Salivary glands (acinar and some duct cells)
 - Lacrimal glands

Thomas J.W. Klein Nulent. *Oral Surg Oral Med Oral Pathol Oral Radiol.* 2018

Modified graphic of original schematic (courtesy of Dr. P.L. Choyke, NCI)

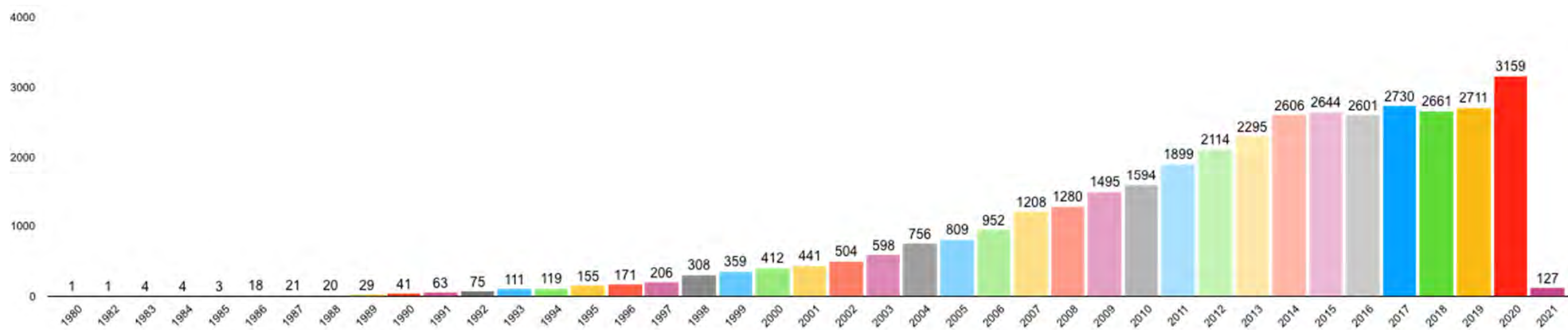


“PSMA PET” publications (source: PubMed)



Society of Nuclear Medicine and Molecular Imaging

“FDG PET” publications (source: PubMed)

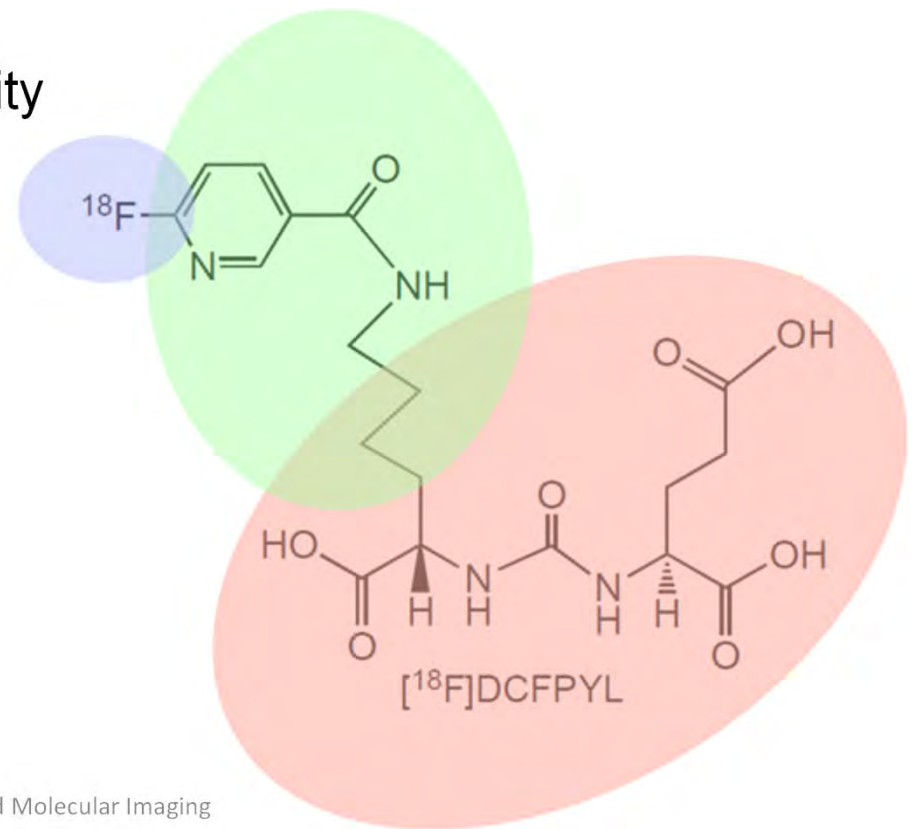


Society of Nuclear Medicine and Molecular Imaging

PyL (¹⁸F DCFPyL)

2-(3-{1-Carboxy-5-[(6-[¹⁸F]fluoro-pyridine-3-carbonyl)-amino]-pentyl}-ureido)-pentanedioic acid

- Developed at Johns Hopkins University by Martin Pomper, MD, PhD
- Prostate Surface Membrane Antigen ligand (PSMA)



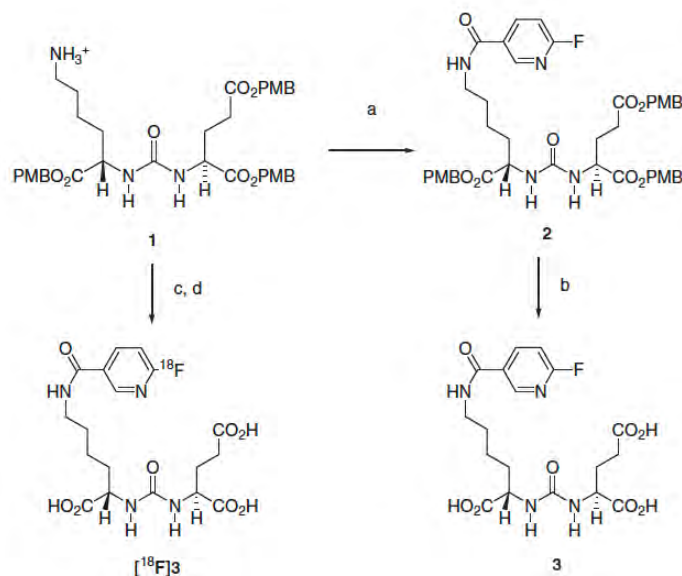
Imaging, Diagnosis, Prognosis

2-(3-{1-Carboxy-5-[(6-[¹⁸F]Fluoro-Pyridine-3-Carbonyl)-Amino]-Pentyl}-Ureido)-Pentanedioic Acid, [¹⁸F]DCFPyL, a PSMA-Based PET Imaging Agent for Prostate Cancer

Ying Chen¹, Mrudula Pullambhatla¹, Catherine A. Foss¹, Youngjoo Byun^{1,2}, Sridhar Nimmagadda¹, Srinivasan Senthamizhchelvan¹, George Sgouros¹, Ronnie C. Mease¹, and Martin G. Pomper¹

Translational Relevance

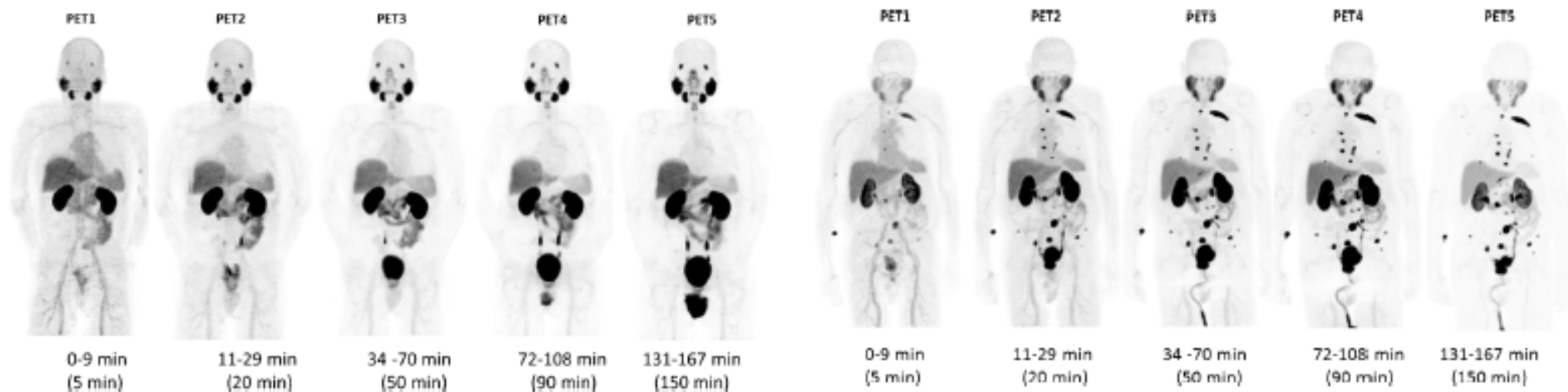
Relative to other malignancies, prostate cancer (PCa) is an elusive target for molecular imaging. By targeting the prostate-specific membrane antigen (PSMA), [¹⁸F]DCFPyL may provide insight into prognosis and androgen receptor (AR) signaling—an important target in PCa research—as well as a way to image locally invasive disease and metastases. The initial indications for [¹⁸F]DCFPyL will be in staging of patients with PCa diagnosed at biopsy or who present with a rising prostate-specific antigen (PSA) blood test after prostatectomy. Other indications include therapeutic monitoring in the context of standard chemotherapeutic agents, AR-based agents and possibly for emerging PSMA-based therapeutics. The superior pharmacokinetics of this compound, namely the high uptake in tumor versus nontarget tissues, the fact that it is a low molecular weight agent, that it can be radiolabeled with a widely available isotope (¹⁸F), and its tractable radiation dosimetry profile all point toward rapid clinical translation through the exploratory Investigational New Drug (eIND) mechanism.



RESEARCH ARTICLE

Initial Evaluation of [¹⁸F]DCFPyL for Prostate-Specific Membrane Antigen (PSMA)-Targeted PET Imaging of Prostate Cancer

Zsolt Szabo,¹ Esther Mena,¹ Steven P. Rowe,¹ Donika Plyku,¹ Rosa Nidal,² Mario A. Eisenberger,² Emmanuel S. Antonarakis,² Hong Fan,¹ Robert F. Dannals,¹ Ying Chen,¹ Ronnie C. Mease,^{1,2} Melin Vranesic,¹ Akrita Bhatnagar,¹ George Sgouros,^{1,2} Steve Y. Cho,^{1,3} Martin G. Pomper^{1,2}



Semiquantitative Parameters in PSMA-Targeted PET Imaging with ^{18}F -DCFPyL: Variability in Normal-Organ Uptake

Xin Li^{1,2}, Steven P. Rowe¹, Jeffrey P. Leal¹, Michael A. Gorin³, Mohamad E. Allaf³, Ashley E. Ross³, Kenneth J. Pienta^{3,4}, Martin A. Lodge¹, and Martin G. Pomper¹

THE JOURNAL OF NUCLEAR MEDICINE • Vol. 58 • No. 6 • June 2017

TABLE 1
SUV_{mean} and SUL_{mean} for Each Organ Across All Patients

Organ	SUV _{mean}	SUL _{mean}
Right lacrimal gland	6.6 ± 1.8	4.9 ± 1.3
Left lacrimal gland	6.4 ± 1.8	4.8 ± 1.3
Right parotid gland	9.1 ± 2.0	6.8 ± 1.6
Left parotid gland	9.0 ± 2.1	6.7 ± 1.7
Right submandibular gland	9.6 ± 2.3	7.1 ± 1.6
Left submandibular gland	9.4 ± 2.2	6.9 ± 1.6
Liver	5.0 ± 0.7	3.8 ± 0.5
Spleen	4.0 ± 1.5	2.9 ± 1.1
Right kidney	20.1 ± 4.6	14.8 ± 3.4
Left kidney	19.4 ± 4.5	14.3 ± 3.3

Data are average and SD of uptake parameters.

TABLE 2
COVs for SUV_{mean} and SUL_{mean} for Each Organ Across All Patients

Organ	SUV _{mean}	SUL _{mean}
Right lacrimal gland	26.9%	26.3%
Left lacrimal gland	27.6%	26.5%
Right parotid gland	22.0%	23.5%
Left parotid gland	23.3%	24.5%
Right submandibular gland	24.3%	23.3%
Left submandibular gland	23.5%	23.7%
Liver	13.8%	14.5%
Spleen	38.7%	38.8%
Right kidney	23.1%	22.6%
Left kidney	23.2%	22.7%

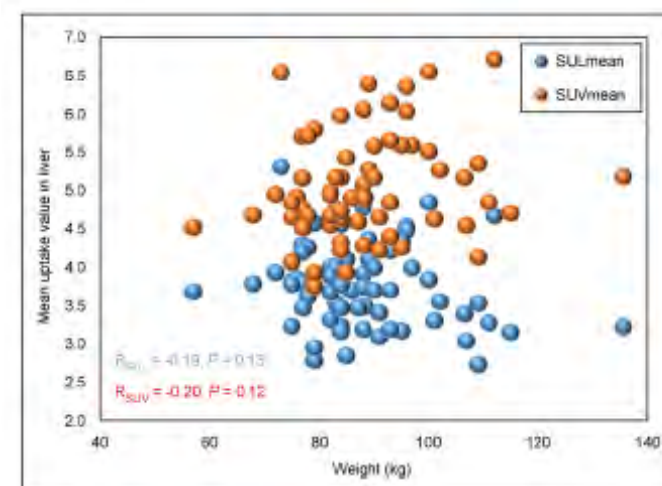


FIGURE 3. Scatterplots of SUV_{mean} and SUL_{mean} in liver against body mass. SUV_{mean} in liver had no significant correlation with mass based on Pearson analysis ($r = 0.195, P = 0.119$). There was also no significant correlation between SUL_{mean} in liver and body mass ($r = -0.19, P = 0.13$).

Simplified Methods for Quantification of ^{18}F -DCFPyL Uptake in Patients with Prostate Cancer

Bernard H.E. Jansen^{1,2}, Maqsood Yaqub¹, Jens Voortman³, Matthijs C.F. Cysouw^{1,3}, Albert D. Windhorst¹, Robert C. Schuit¹, Gerbrand M. Kramer¹, Alfons J.M. van den Eertwegh³, Lothar A. Schwarte⁴, N. Harry Hendrikse^{1,4}, André N. Vis³, Reindert J.A. van Moorselaar², Otto S. Hoekstra¹, Ronald Boellaard¹, and Daniela E. Oprea-Lager¹

THE JOURNAL OF NUCLEAR MEDICINE • Vol. 60 • No. 12 • December 2019

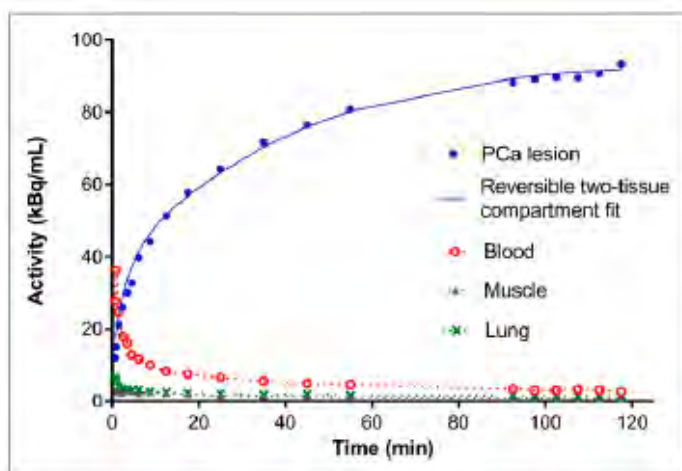


FIGURE 2. Typical example of ^{18}F -DCFPyL uptake in a PCa metastasis (including fit from reversible 2-tissue-compartment model with fixed k_4), blood, muscle, and lung.

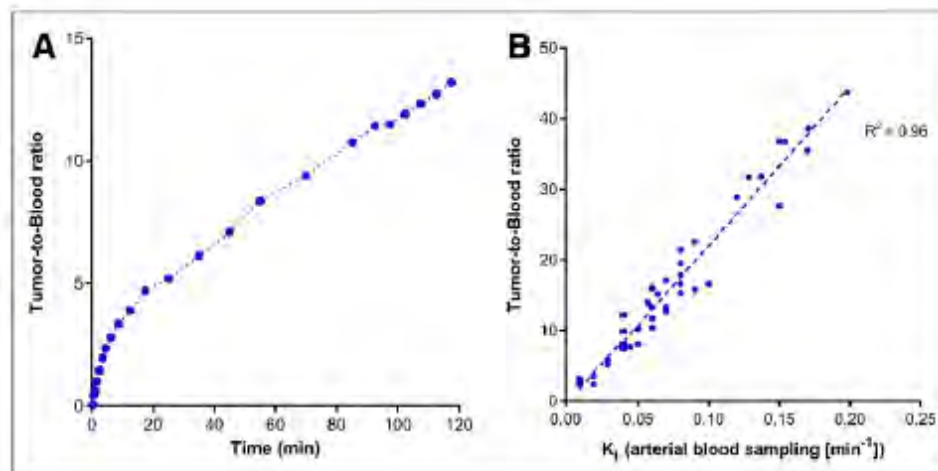


FIGURE 3. (A) Example of typical TBR over time. (B) Correlation of image-based TBRs and K_1 derived from pharmacokinetic modeling (reversible 2-tissue-compartment model).

Repeatability of Quantitative ^{18}F -DCFPyL PET/CT Measurements in Metastatic Prostate Cancer

Bernard H.E. Jansen^{1,2}, Matthijs C.F. Cysouw^{1,3}, André N. Vis², Reindert J.A. van Moorselaar², Jens Voortman³, Yves J.L. Bodar^{1,2}, Patrick R. Schober⁴, N. Harry Hendrikse^{1,5}, Otto S. Hoekstra¹, Ronald Boellaard¹, and D.E. Oprea-Lager¹

THE JOURNAL OF NUCLEAR MEDICINE • Vol. 61 • No. 9 • September 2020

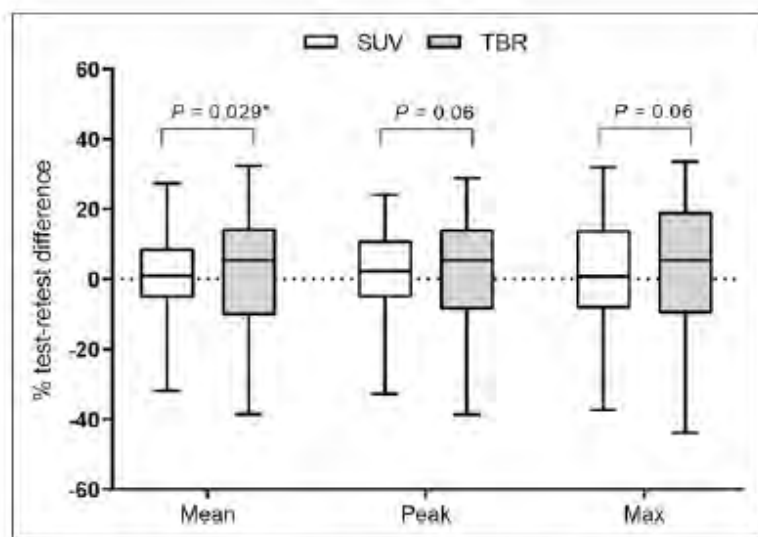


FIGURE 1. Test-retest variability of SUV and TBR variants. Significant differences have been indicated with asterisk (Holms-Bonferroni-corrected *P* values). Differences in repeatability between SUVs and between TBRs were not significant.

TABLE 3
Repeatability of Lesion- and Patient-Based ^{18}F -DCFPyL Uptake Metrics

Parameter	Mean test-retest difference (%)	RC (%)	ICC	95% CI
Lesion level				
Volume	-1.1	28.1	1.00	0.99-1.00
SUV _{mean}	1.0	24.4	0.99	0.98-0.99
SUV _{peak}	1.8	25.3	0.99	0.97-0.99
SUV _{max}	1.9	31.0	0.97	0.94-0.99
Mean TBR	1.9	31.8	0.98	0.96-0.99
Peak TBR	2.6	31.7	0.98	0.96-0.99
Maximum TBR	2.7	37.3	0.97	0.94-0.98
SUV TLU	-0.1	32.1	0.99	0.98-1.00
TBR TLU	-3.5	39.3	0.98	0.96-0.99
Patient level				
TTV	-2.2	17.0	1.00	0.99-1.00
SUV TTB	-0.2	23.2	0.99	0.97-1.00
TBR TTB	-2.1	33.4	0.98	0.91-0.99

ICC = intraclass correlation coefficient; CI = confidence interval.

Semiquantitative Parameters in PSMA-Targeted PET Imaging with [¹⁸F]DCFPyL: Impact of Tumor Burden on Normal Organ Uptake

Rudolf A. Werner,^{1,2,3,4} Ralph A. Bundschuh,⁵ Lena Bundschuh,⁵ Constantin Lapa,² Yafu Yin,^{1,6,7} Mehrbod S. Javadi,¹ Andreas K. Buck,^{2,3} Takahiro Higuchi,^{2,3,8} Kenneth J. Pienta,⁹ Martin G. Pomper,^{1,9} Martin A. Lodge,¹ Michael A. Gorin,^{1,9} Steven P. Rowe^{1,9,10}

Mol Imaging Biol. 2020 February ; 22(1): 190–197.

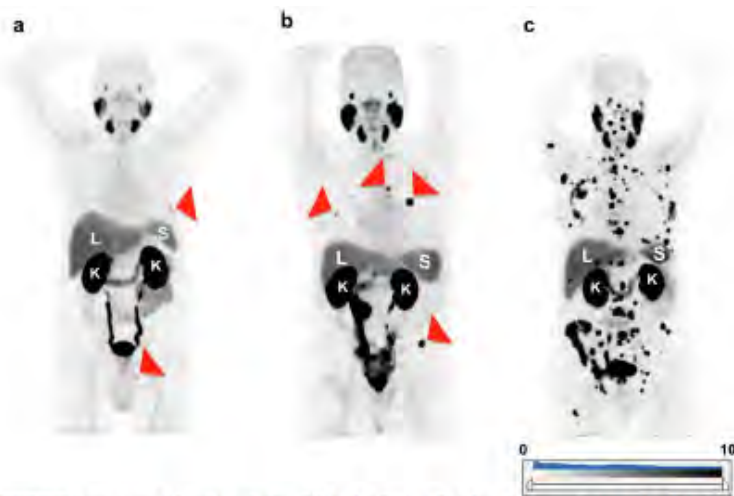


Fig. 2. [¹⁸F]DCFPyL maximum intensity projection (MIP) of patients with a low, b intermediate, and c high tumor burden. Spleen (S), liver (L), and kidneys (K) are indicated. Red arrows indicate representative tumor lesions, which can be detected on the MIPs: In patient a: metastases in the seventh rib (left) and in the left ischium are indicated. In patient b: multiple bone lesions are indicated. Patient c shows a near-superscan with extensive involvement in the skeleton. The uptake in normal organs (visible for liver, kidneys, and spleen) does not differ visually among the different patients.

Table 2. Descriptive statistics of normal organs and tumor burden

Compartment	Parameter	Minimum	Median	Maximum	Mean*	StDev*
Lacrimal gland L	SUL _{mean}	1.8	3.6	5.2	3.7	0.7
	SUV _{max}	2.4	4.9	6.7	5	0.9
Lacrimal gland R	SUL _{mean}	2.4	3.7	5.6	3.7	0.7
	SUV _{max}	3.3	5.1	7	5.1	0.9
Parotid gland L	SUL _{mean}	3	6	11.1	6.2	1.9
	SUV _{max}	5	8.1	13.8	8.3	2.4
Parotid gland R	SUL _{mean}	2	6.3	11.3	6.3	1.9
	SUV _{max}	4.9	8.2	14.2	8.5	2.4
SMG L	SUL _{mean}	3.3	5.8	13.5		
	SUV _{max}	5	7.9	17.5		
SMG R	SUL _{mean}	1.9	5.9	13.1		
	SUV _{max}	4	8	16.8		
Liver	SUL _{mean}	2.6	3.7	4.7	3.7	0.5
	SUV _{max}	3.5	5	6.3	5	0.7
Spleen	SUL _{mean}	0.8	2.6	7.8		
	SUV _{max}	1.3	3.7	14.4		
Kidney L	SUL _{mean}	7.8	16.6	28.7	17.4	5
	SUV _{max}	10.5	22.8	41.3		
Kidney R	SUL _{mean}	11.4	17.3	30.9	18.1	5
	SUV _{max}	11.2	23.4	43.6		
Tumor burden	SUL _{mean}	1.3	3.9	42.9		
	SUL _{max}	1.7	5.3	55.6		
	SUV _{max}	1.6	5.4	57.9		
	TV	0.3	4.8	98.4		
	FTA	1.0	25.9	1752		

SUL_{mean} mean standardized uptake value corrected to lean body mass, SUV_{max} mean standardized uptake value corrected to body weight, SMG submandibular gland, SUL_{max} the maximum standardized uptake value corrected to lean body mass, TV tumor volume (in ml), FTA fractional tumor activity in the volume of interest, L left, R right

*Mean and standard deviation (StDev) are not shown when the Shapiro-Wilk test excluded a normal distribution

Pelvic lymph-node staging with ^{18}F -DCFPyL PET/CT prior to extended pelvic lymph-node dissection in primary prostate cancer - the SALT trial -

B. H. E. Jansen^{1,2,3}  • Y. J. L. Bodar^{1,2,3}  • G. J. C. Zwezerijnen² • D. Meijer^{1,2,3} • J. P. van der Voorn⁴ • J. A. Nieuwenhuijzen^{1,3} • M. Wondergem⁵ • T. A. Roeleveld^{3,6} • R. Boellaard² • O. S. Hoekstra² • R. J. A. van Moorselaar^{1,3} • D. E. Oprea-Lager² • A. N. Vis^{1,3}

Table 3 The diagnostic value of ^{18}F -DCFPyL PET/CT for detecting lymph-node metastatic disease on a per-patient and template basis

Patient-based accuracy					
	pN1	pN0	Total	% (95%CI)	
cN1	7	6	13	53.8 (26.1–79.6)	PPV
cN0	10	94	104	90.4 (82.6–95.0)	NPV
Total	17	100	117	14.5	Prevalence
% (95%CI)	41.2 (19.4–66.5)	94.0 (86.9–97.5)			
	Sensitivity	Specificity			
Template-based accuracy					
	pN1	pN0	Total	% (95%CI)	
cN1	8	10	18	44.4 (22.4–68.6)	PPV
cN0	15	435	450	96.6 (94.4–98.0)	NPV
Total	23	445	468	4.9	Prevalence
% (95%CI)	34.7 (17.1–57.1)	97.7 (95.7–98.9)			
	Sensitivity	Specificity			

Prospective Evaluation of ^{18}F -DCFPyL PET/CT in Biochemically Recurrent Prostate Cancer in an Academic Center: A Focus on Disease Localization and Changes in Management

THE JOURNAL OF NUCLEAR MEDICINE • Vol. 61 • No. 4 • April 2020

Hong Song, Caitlyn Harrison, Heying Duan, Kip Guja, Negin Hatami, Benjamin L. Franc, Farshad Moradi, Carina Mari Aparici, Guido A. Davidzon, and Andrei Iagaru

TABLE 1
Demographics and Characteristics of Participants

Characteristic	Data
Age (y), mean \pm SD	71.5 \pm 7.2
Primary definitive treatment (n)	
Radical prostatectomy	42 (58%)*
Radiation therapy	30 (42%)
Gleason score at initial diagnosis (n)	
6	6 (8%)
7	37 (51%)
8	11 (15%)
9	17 (24%)
10	1 (1%)
Median time to first BCRT* (mo)	
Radical prostatectomy	36 (range, 3–120)
Radiation therapy	48 (range, 4–192)
^{18}F -DCFPyL activity (MBq), mean \pm SD	338.8 \pm 25.3
Time to acquisition after injection (min), mean \pm SD	74.4 \pm 10.4

TABLE 2
Positivity Rates of ^{18}F -DCFPyL PET/CT Based on PSA Level and PSA Doubling Time

PSA parameter	Positive scan (n)	Negative scan (n)	Percentage positive
Level (ng/mL)			
PSA < 0.5	4	4	50%
0.5 \leq PSA < 1	9	4	69%
1 \leq PSA < 2	5	0	100%
2 \leq PSA < 5	20	2	91%
PSA \geq 5	23	1	96%
Total	61	11	85%
Doubling time (mo)*			
0–3	13	2	87%
3–6	17	3	85%
6–12	11	1	92%
>12	11	3	79%

Number of ¹⁸F-DCFPyL positive lesions

Number of lesions	Number of lesions prostate bed	Lymph nodes pelvic	Lymph nodes extra-pelvic	Bones	Other organs ^a
Radical Prostatectomy	21	226	260	325	57
Radiation therapy	36	104	216	293	44

^a Most commonly in the lungs.

Sites of metastatic lesions that can be candidates for local targeted therapy

	Prostate bed only	Pelvic only (Prostate bed with or without pelvic lymph nodes)	Extra-Pelvic Oligometastases (1-3)
Number of Patients (%)	25 (14)	45 (25)	53 (29)

Impact of ¹⁸F DCFPyL PET/CT on patient management

Number of patients (% total patients)	Positive DCFPyL PET	Negative ^b DCFPyL PET
Treatment after DCFPyL PET/CT	108 (60)	8 (4)
Radiation +/- ADT	64 (35)	6 (3)
ADT	44 (24)	2 (1)
Surveillance	14 (8)	17 (9)
Other	29 ^a (16)	

^a 20 patients had no documented management plan. 3 patients started ADT before the scan and continued afterwards

^b 8 patients received empirical treatment despite negative DCFPyL PET findings.

A Phase 2/3 Prospective Multicenter Study of the Diagnostic Accuracy of Prostate-Specific Membrane Antigen PET/CT with ^{18}F -DCFPyL In Prostate Cancer Patients (OSPNEY)

¹Kenneth J. Pienta, MD, ^{1,2}Michael A. Gorin, MD, ²Steven P. Rowe, MD, PhD, ³Peter R. Carroll, MD, ⁴Frédéric Pouliot, MD, PhD, ⁵Stephan Probst, MD, ⁶Lawrence Saperstein, MD, ⁷Mark A. Preston, MD, MPH, ⁸Ajjai S. Alva, MD, ⁹Akash Patnaik, MD, PhD, ¹⁰Jeremy C. Durack, MD, ¹¹Nancy Stambler, DrPH, ¹¹Tess Lin, PharmD, ¹¹Jessica Jensen, MPH, ¹¹Vivien Wong, PhD, ¹²Barry A. Siegel, MD, ^{10,13}Michael J. Morris, MD and OSPNEY Study Group*


CLINICAL CANCER RESEARCH

[Home](#) [About](#) [Articles](#) [For Authors](#) [Alerts](#) [News](#) [COVID-19](#) [Webinars](#) [Search Q](#)

Research Article

Diagnostic Performance of ^{18}F -DCFPyL-PET/CT in Men with Biochemically Recurrent Prostate Cancer: Results from the CONDOR Phase 3, Multicenter Study

Michael J. Morris, Steven P. Rowe, Michael A. Gorin, Lawrence Saperstein, Frédéric Pouliot, David Y Josephson, Jeffrey YC Wong, Austin R Pantel, Steve Y Cho, Kenneth L Gage, Morand R Piert, Andrei Iagaru, Janet H. Pollard, Vivien Wong, Jessica Jensen, Tess Lin, Nancy Stambler, Peter Carroll, and Barry A Siegel

DOI: 10.1158/1078-0432.CCR-20-4573  Check for updates

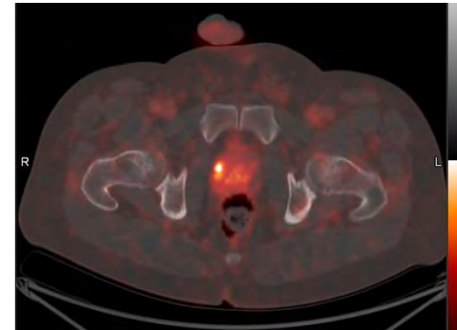
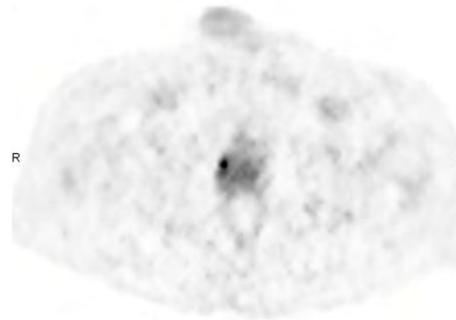
Society of Nuclear Medicine and Molecular Imaging

Scanning Protocols

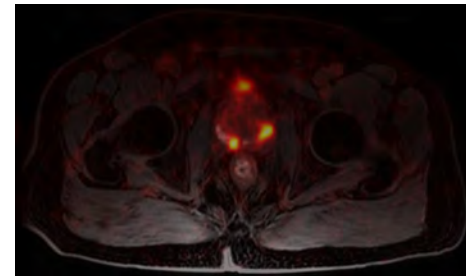
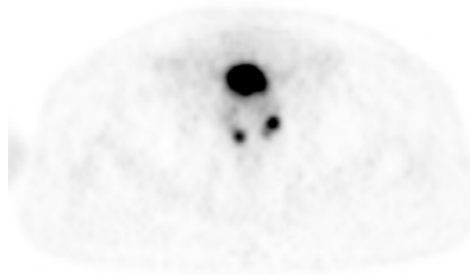
Society of Nuclear Medicine and Molecular Imaging

Positron Emission Tomography (PET) Cameras

PET/CT system and images



PET/MRI system and images



Effects of Fasting on ^{18}F -DCFPyL Uptake in Prostate Cancer Lesions and Tissues with Known High Physiologic Uptake

Maurits Wondergem¹, Friso M. van der Zant¹, Peter W. Vlottes², and Remco J.J. Knol¹

J Nucl Med 2018; 59:1081–1084

TABLE 2
Comparison of ^{18}F -DCFPyL Uptake

Tissue	Cohort	Minutes after injection	n	SUV _{max}	P
Malignant lesions	Fasting	60	152	10.2	0.420
	Nonfasting		131	10.5	
	Fasting	120	152	12.5	
	Nonfasting		131	12.8	
Submandibular gland*	Fasting	60	50	16.2	0.017
	Nonfasting		47	18.7	
	Fasting	120			
	Nonfasting				
Liver	Fasting	60	50	6.8	<0.001
	Nonfasting		48	7.7	
	Fasting	120	50	6.9	
	Nonfasting		48	7.9	
Spleen	Fasting	60	48	5.6	0.035
	Nonfasting		47	6.4	
	Fasting	120	48	4.6	
	Nonfasting		47	4.8	
Duodenum	Fasting	60	50	11.4	0.013
	Nonfasting		48	13.3	
	Fasting	120	50	13.3	
	Nonfasting		48	14.6	
Intestine (other)	Fasting	60	38	4.3	0.116
	Nonfasting		38	4.9	
	Fasting	120	38	3.8	
	Nonfasting		38	5.5	

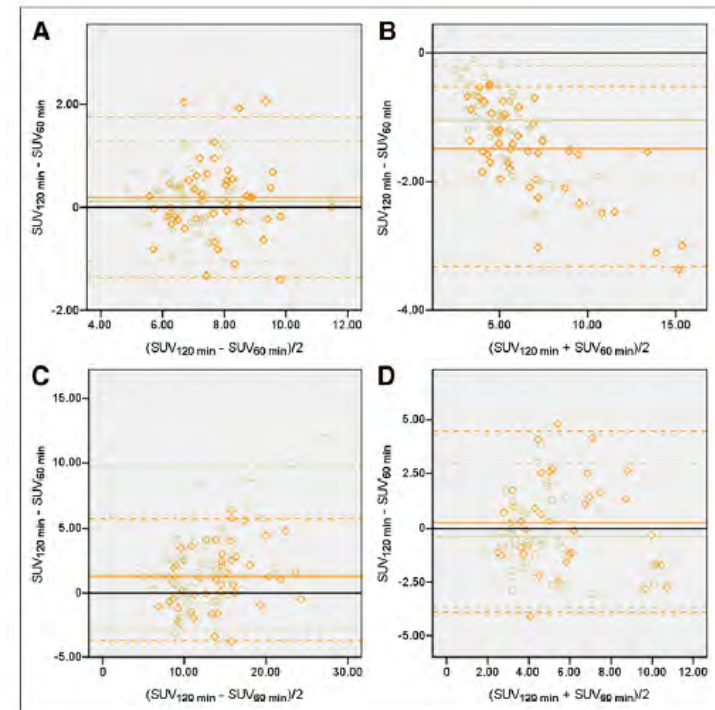


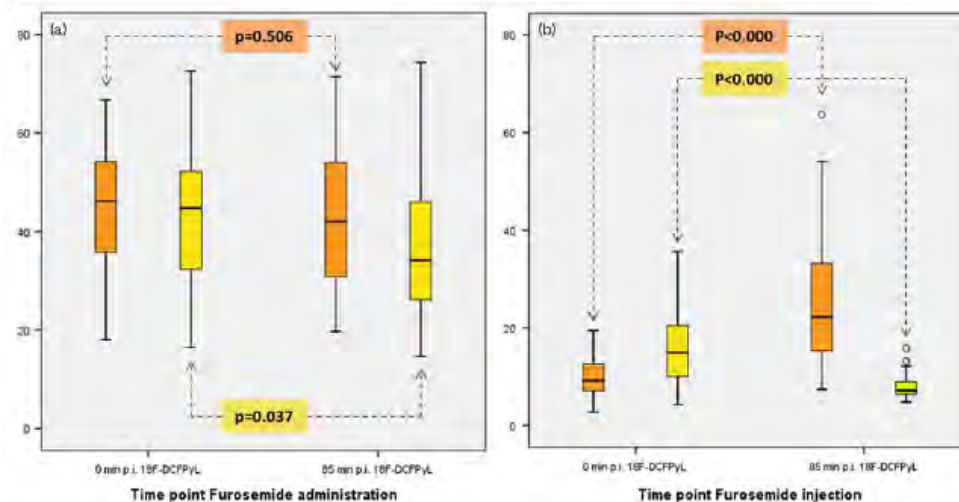
FIGURE 2. Difference between ^{18}F -DCFPyL activity at 120 and 60 min after injection plotted against mean activity in liver (A), spleen (B), duodenum (C), and other intestinal locations (D) in fasting (○) and nonfasting (◇) cohorts.

Effect of forced diuresis during ^{18}F -DCFPyL PET/CT in patients with prostate cancer: activity in ureters, kidneys and bladder and occurrence of halo artefacts around kidneys and bladder

Maurits Wondergem, Friso M. van der Zant, Ladan Rafimanesh-Sadr and Remco J.J. Knol

Nuclear Medicine Communications 2019, 40:652–656

Fig. 2

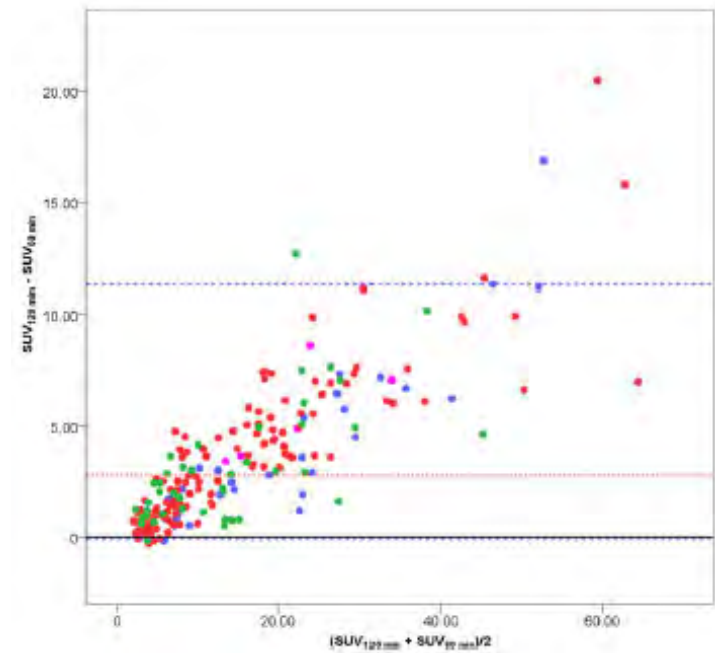
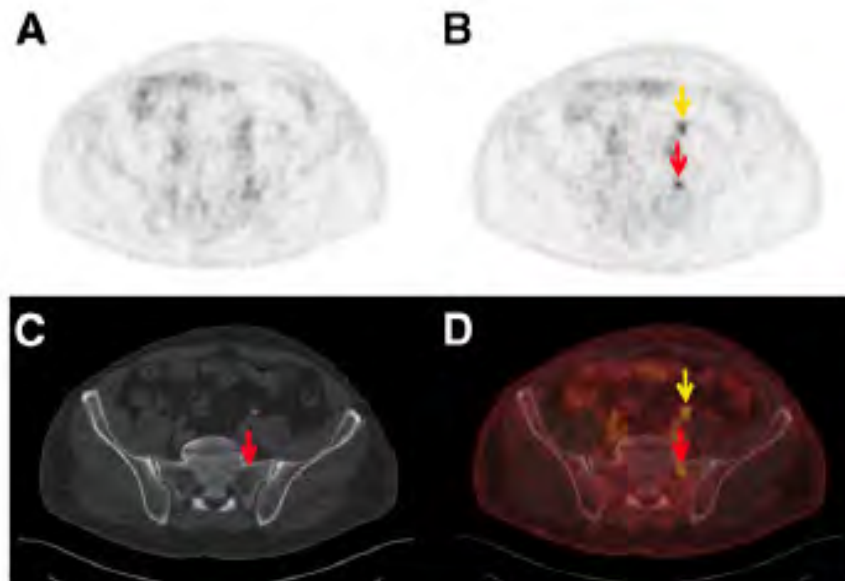


Boxplots of measured ^{18}F -DCFPyL activity (maximum standardized uptake value) in kidneys (a) and bladder (b) at images 60 min (orange boxplots) and 120 min (yellow boxplots) after ^{18}F -DCFPyL administration for both the cohort that received furosemide simultaneously with ^{18}F -DCFPyL and the cohort that received furosemide 85 min after ^{18}F -DCFPyL administration. ^{18}F -DCFPyL, 2-(3-(1-carboxy-5-((6- ^{18}F)fluoro-pyridine-3-carbonyl)-amino)-pentyl)-ureido)-pentanedioic acid.

^{18}F -DCFPyL PET/CT in the Detection of Prostate Cancer at 60 and 120 Minutes: Detection Rate, Image Quality, Activity Kinetics, and Biodistribution

Maurits Wondergem^{1,2}, Friso M. van der Zant¹, Remco J.J. Knol¹, Sergiy V. Lazarenko¹, Jan Pruim^{3,4}, and Igle J. de Jong²

J Nucl Med 2017; 58:1797–1804



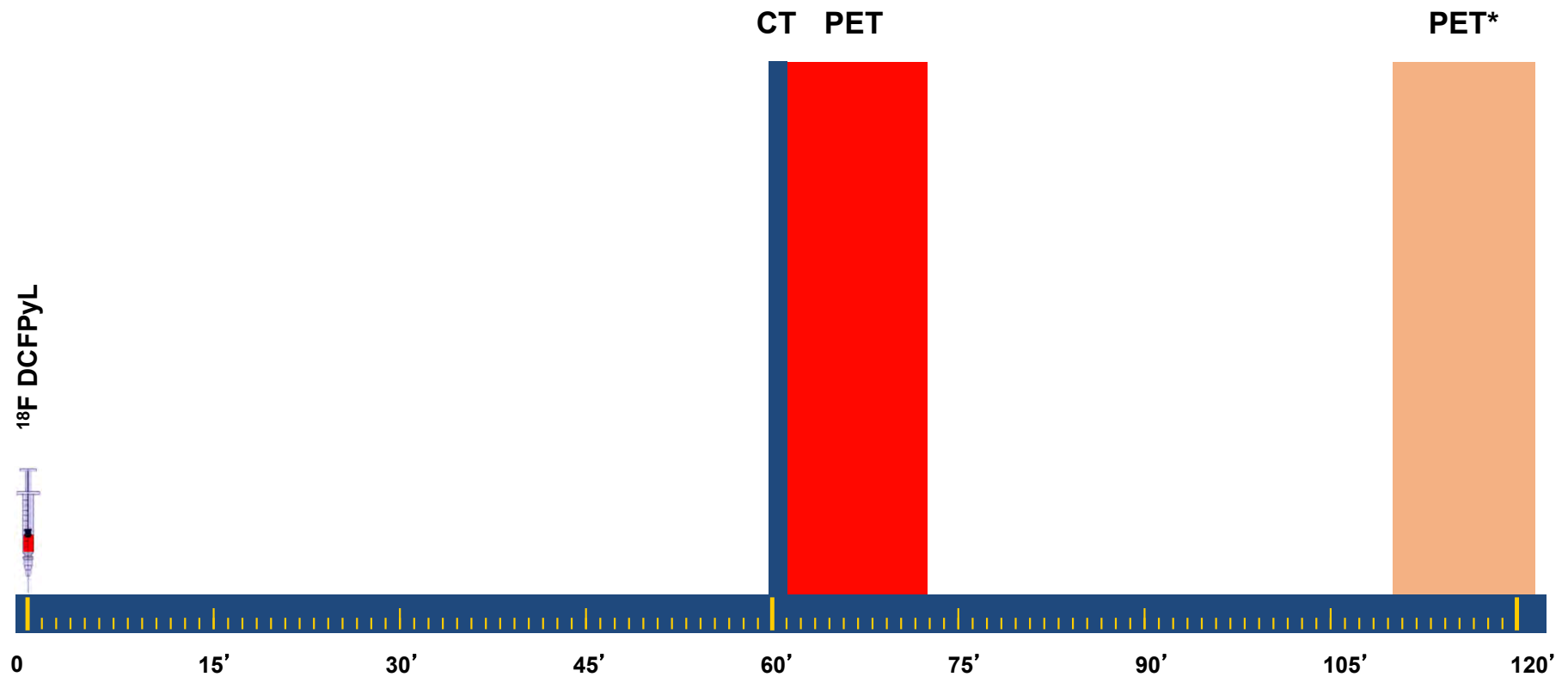
Patient Preparation

- There is no fasting requirement prior to the ^{18}F -DCFPyL injection
- Instruct patient to drink water (1-2 glasses) to ensure adequate hydration prior to the administration of ^{18}F -DCFPyL

Voiding

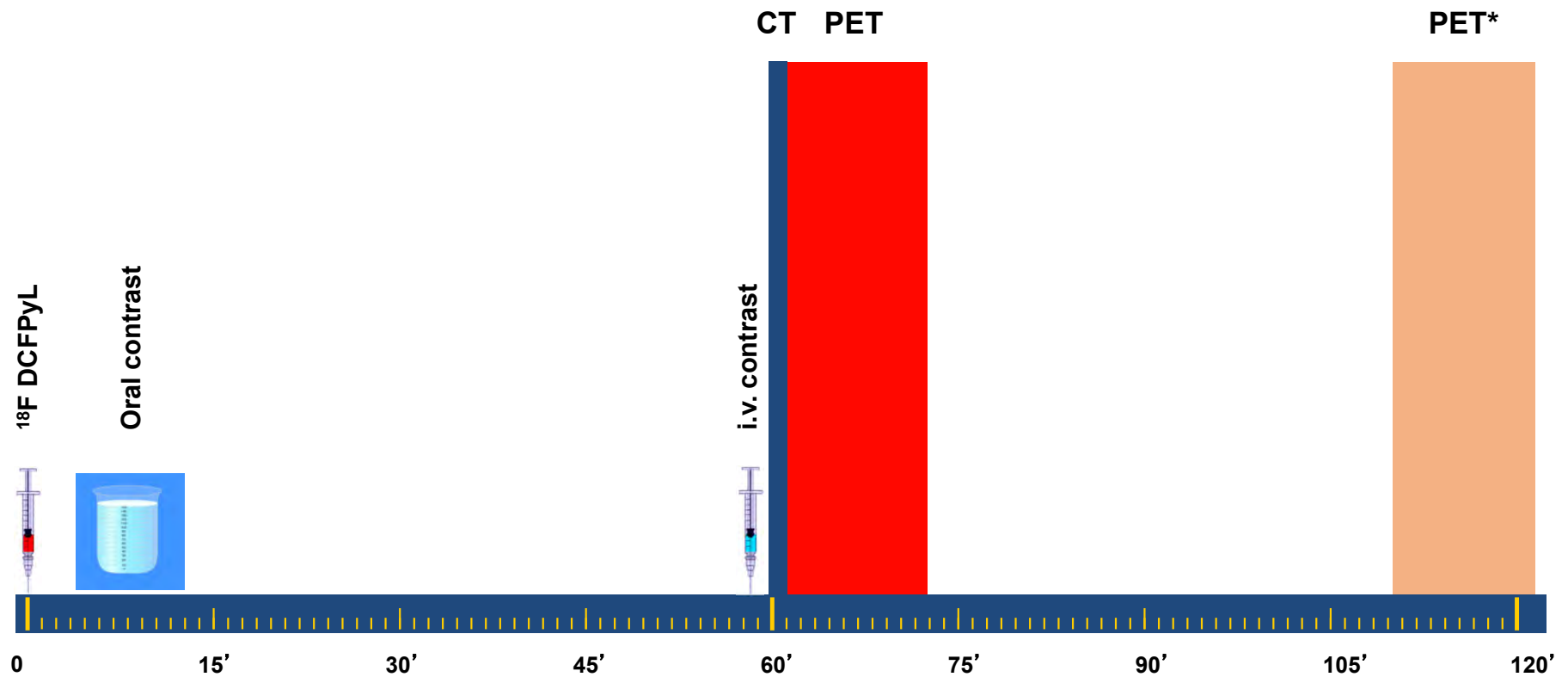
- Instruct patients to void frequently for the first few hours following administration of ^{18}F -DCFPyL to reduce radiation exposure, including during uptake and immediately prior to scanning

Initial Staging (Pre-Prostatectomy) and Biochemical Recurrence



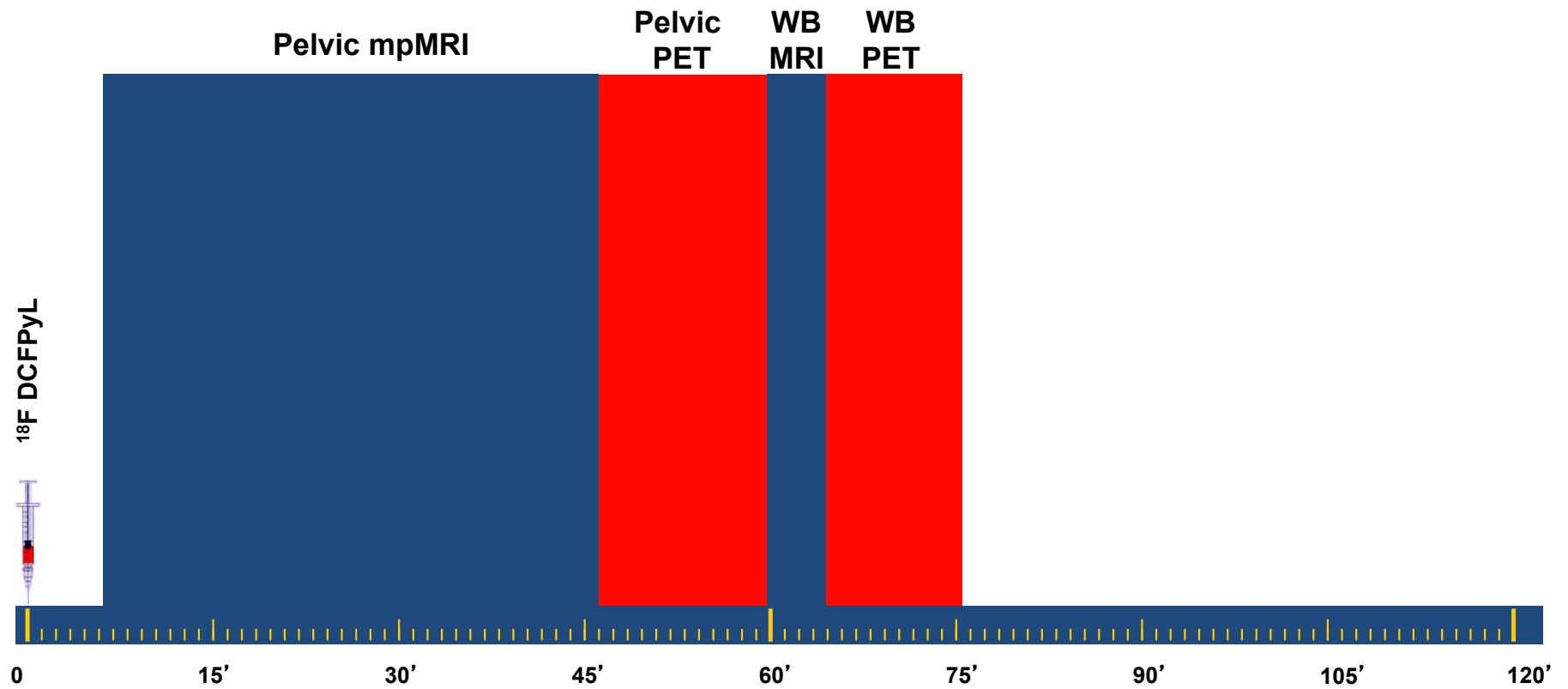
*Delayed PET images at 120 mins post-injection may identify additional lesions.

Initial Staging (Pre-Prostatectomy) and Biochemical Recurrence



*Delayed PET images at 120 mins post-injection may identify additional lesions.

Initial Staging (Pre-Prostatectomy), if PET/MRI available



Standardized Protocols

- ✓ *dosage adjusted per body weight*
- ✓ *time from injection to imaging*
- ✓ *oral contrast*
- ✓ *i.v. contrast*
- ✓ *reporting of CT findings*

^{18}F DCFPyL vs. other PSMA targeting PET radiopharmaceuticals

Intraindividual Comparison of ^{18}F -PSMA-1007 and ^{18}F -DCFPyL PET/CT in the Prospective Evaluation of Patients with Newly Diagnosed Prostate Carcinoma: A Pilot Study

Frederik L. Giesel^{1,2}, Leon Will¹, Ismaheel Lawal³, Thabo Lengana³, Clemens Kratochwil¹, Mariza Vorster³, Oliver Neels⁴, Florette Reyneke³, Uwe Haberkon^{1,2}, Klaus Kopka⁴, and Mike Sathekge³

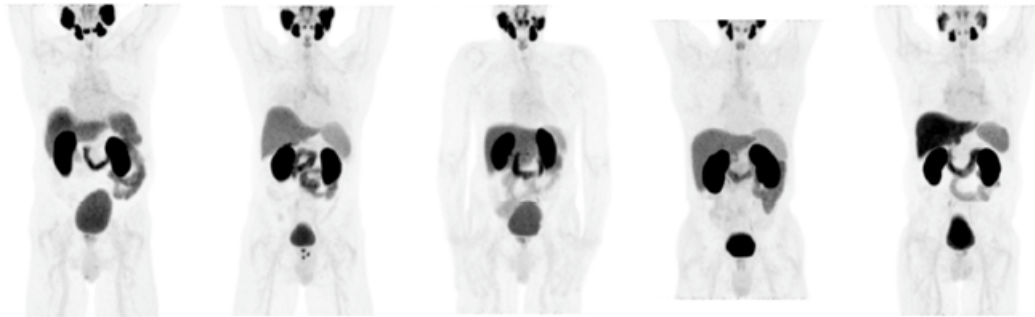
THE JOURNAL OF NUCLEAR MEDICINE • Vol. 59 • No. 7 • July 2018

Matched-pair comparison of ^{18}F -DCFPyL PET/CT and ^{18}F -PSMA-1007 PET/CT in 240 prostate cancer patients; inter-reader agreement and lesion detection rate of suspected lesions.

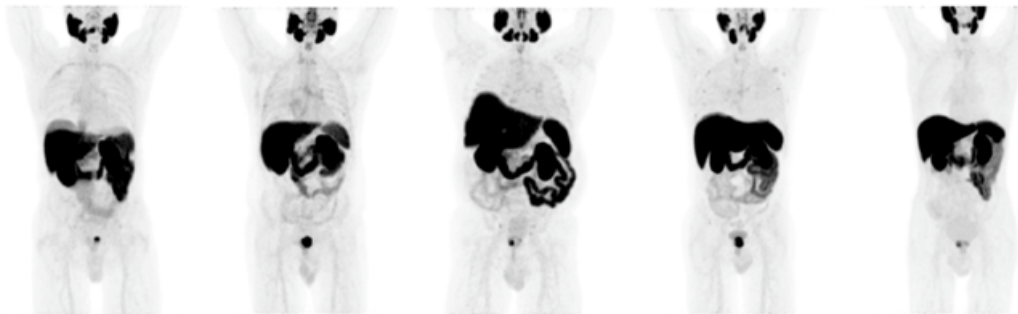
Maurits Wondergem¹, MD, PhD, Friso M. van der Zant¹, MD, PhD, Wouter A.M. Broos¹, MD, Remco J.J. Knol¹, MD, PhD

Journal of Nuclear Medicine, published on February 5, 2021

^{18}F -DCFPyL



^{18}F -PSMA-1007



Comparison of [^{18}F]DCFPyL and [^{68}Ga]Ga-PSMA-HBED-CC for PSMA-PET Imaging in Patients with Relapsed Prostate Cancer

Markus Dietlein,^{1,3} Carsten Kobe,^{1,3} Georg Kuhnert,^{1,3} Simone Stockter,¹ Thomas Fischer,¹ Klaus Schomäcker,¹ Matthias Schmidt,^{1,3} Felix Dietlein,^{1,3} Boris D. Zlatopolskiy,² Philipp Krapf,² Raphael Richarz,² Stephan Neubauer,⁴ Alexander Drzezga,^{1,3} Bernd Neumaier²

Mol Imaging Biol (2015) 17:575–584

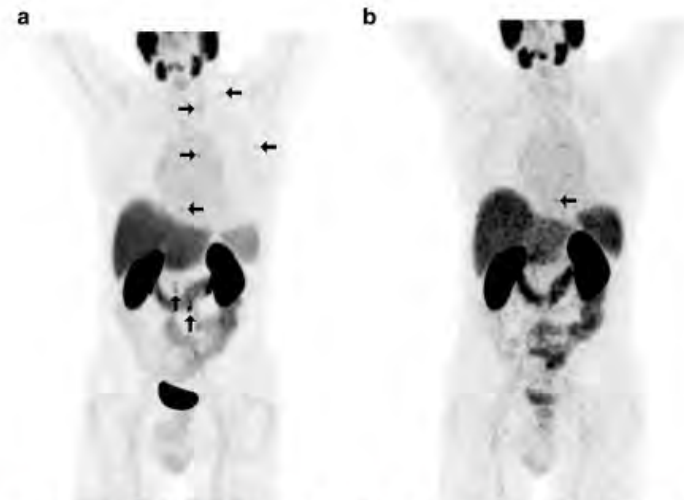


Fig. 1 Patient no. 12 with a rising PSA level of 3.87 ng/ml. In the past, the patient had retroperitoneal lymph node metastases, which were irradiated. On a Biograph mCT 128 scanner, comparison between a MIP (maximum intensity projection) with [^{18}F]DCFPyL and b MIP with [^{68}Ga]Ga-PSMA-HBED-CC. [^{18}F]DCFPyL PET/CT clearly demonstrates several additional supradiaphragmatic PSMA-positive lesions. [^{68}Ga]Ga-PSMA-HBED-CC PET/CT showed the supradiaphragmatic lesion in the sternum.

Uptake in non-affected bone tissue does not differ between [^{18}F]-DCFPyL and [^{68}Ga]-HBED-CC PSMA PET/CT

Jochen Hammes^{1*}, Melanie Hohberg¹, Philipp Täger¹, Markus Wild¹, Boris Zlatopolskiy², Philipp Krapf³, Bernd Neumaier^{2,3}, Klaus Schomäcker¹, Carsten Kobe¹, Matthias Schmidt¹, Markus Dietlein¹, Alexander Drzezga¹

PLOS ONE | <https://doi.org/10.1371/journal.pone.0209613> December 20, 2018

Table 1. Quantitative results in bone negative group. Average values and standard deviation.

	^{18}F -DCFPyL	^{68}Ga -PSMA-HBED-CC	p (Wilcoxon)
SUV _{liver}	6.1 (1.2)	4.6 (1.0)	<0.01*
SUV _{glandulae}	0.35 (0.13)	0.36 (0.08)	0.62
SUV _{bone}	0.49 (0.08)	0.52 (0.06)	0.03*
SUV _{bone} / SUV _{liver}	0.082 (0.02)	0.117 (0.019)	<0.01*
SUV _{bone} / SUV _{glandulae}	1.50 (0.37)	1.54 (0.39)	0.55

* indicates statistical significance

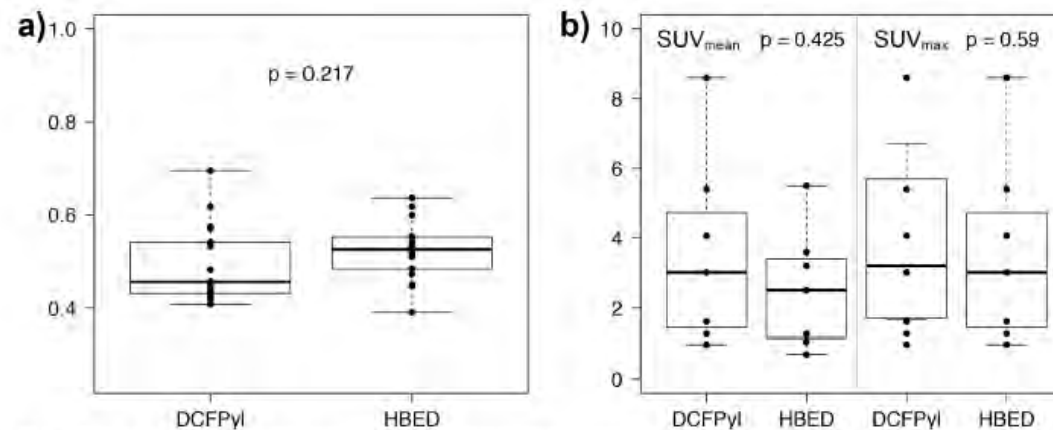


Fig 3. a) Average SUVs in unaffected bone tissue in 17 patients without bone metastases. b) SUV_{mean} and SUV_{max} in a total of seven bone metastases in the group of patients with bone metastases.

Intra-individual comparison of ^{68}Ga -PSMA-11 and ^{18}F -DCFPyL normal-organ biodistribution

Gonalo Ferreira^{1,2*}, Amir Iravani², Michael S. Hofman^{2,3} and Rodney J. Hicks^{2,3}

Cancer Imaging (2019) 19:23

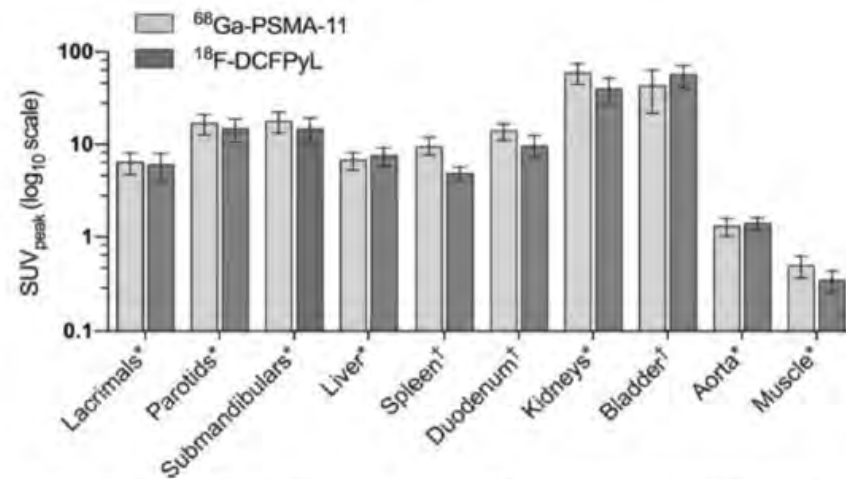
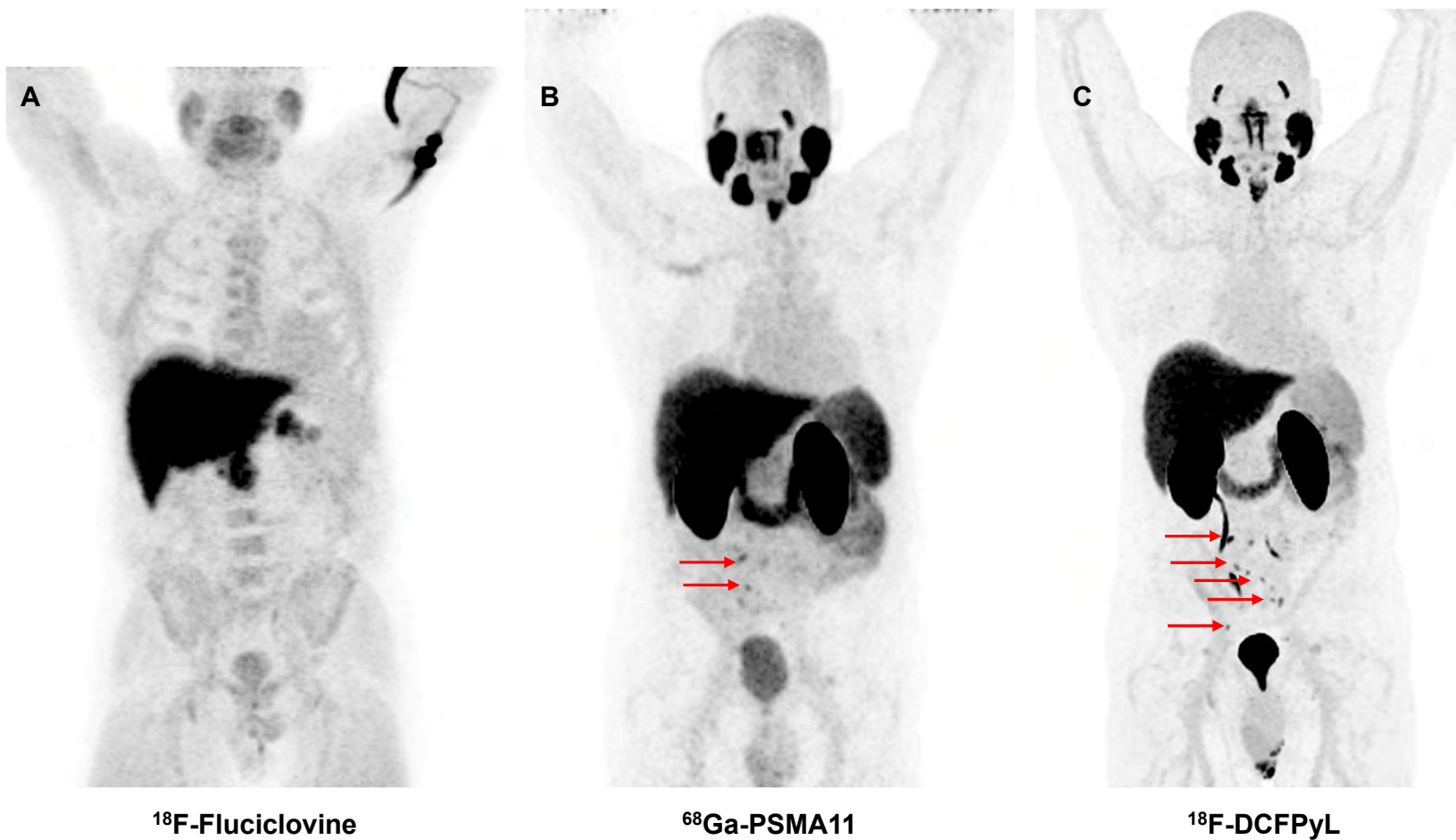


Fig. 2 Clustered bar chart of normal-organ SUV_{peak} with either tracer (^{68}Ga -PSMA-11 and ^{18}F -DCFPyL). For data normally distributed: *mean with standard deviation error bars; for data not normally distributed: †median with interquartile range error bars. Plotted on a logarithmic scale (log₁₀)

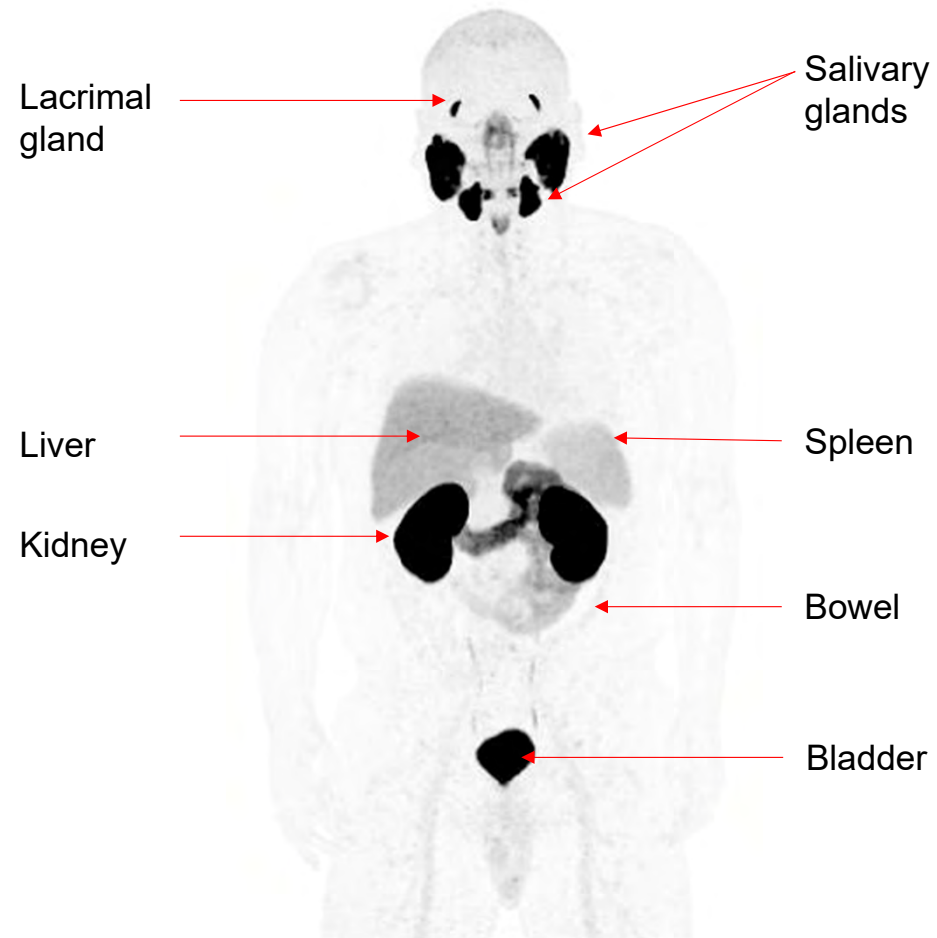


63 year-old man with BCR PC (PSA 3.14) had a ^{18}F -Fluciclovine (A) that was negative, but ^{68}Ga -PSMA11 PET (B) done within 30 days showed pelvic nodal metastases (arrows). ^{18}F -DCFPyL PET (C) done 3 days after ^{68}Ga -PSMA11 showed more extensive nodal metastases (arrows).

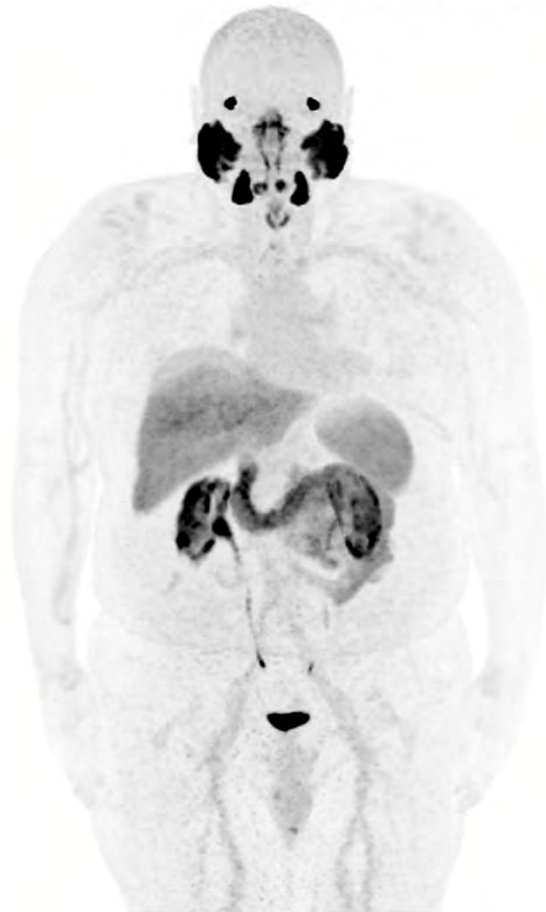
Image Interpretation

Society of Nuclear Medicine and Molecular Imaging

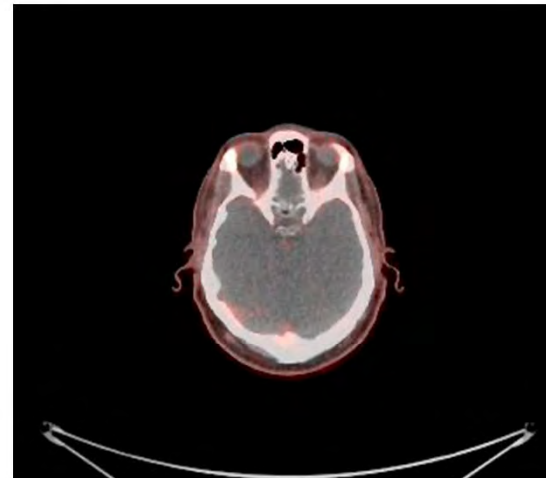
^{18}F -DCFPyL: Normal Biodistribution



^{18}F -DCFPyL: Normal Biodistribution

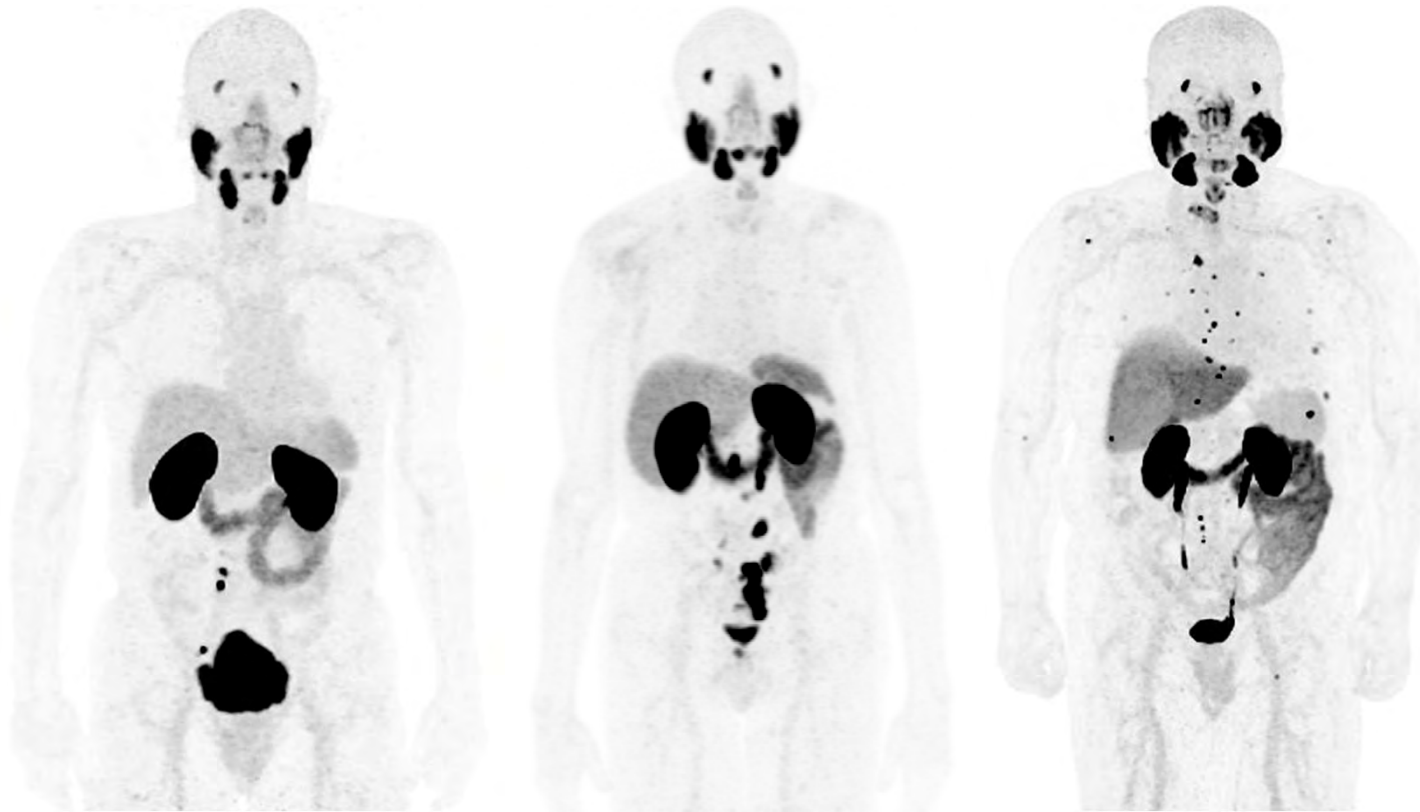


Click on
image
for MIP
video



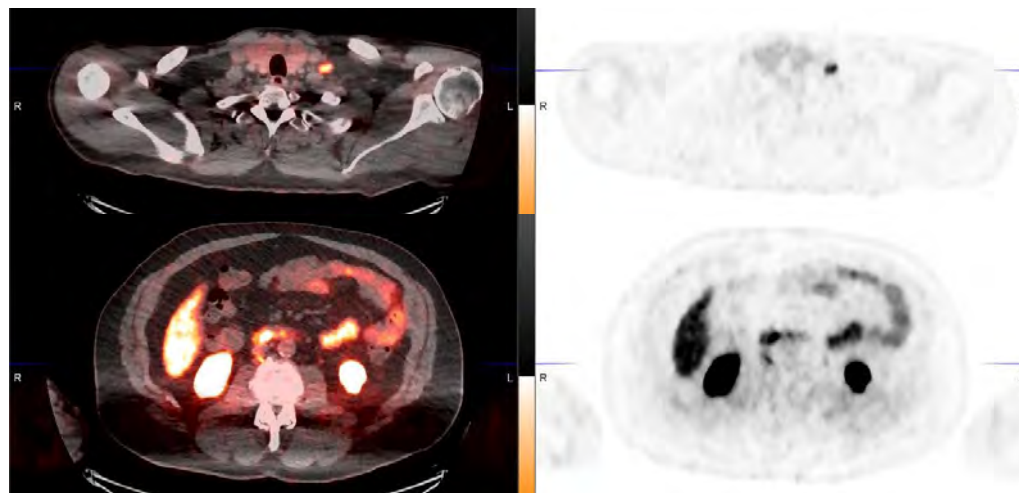
Click on
image
for video
play

Prostate Cancer Lesions



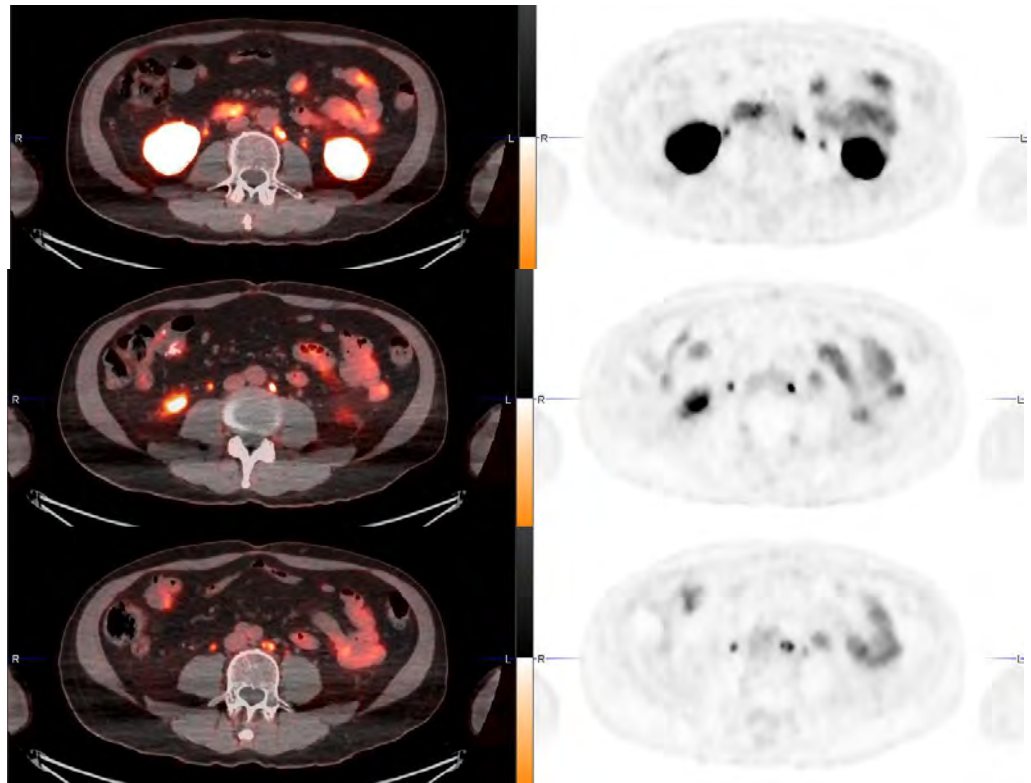
Society of Nuclear Medicine and Molecular Imaging

Click on
image for
MIP video



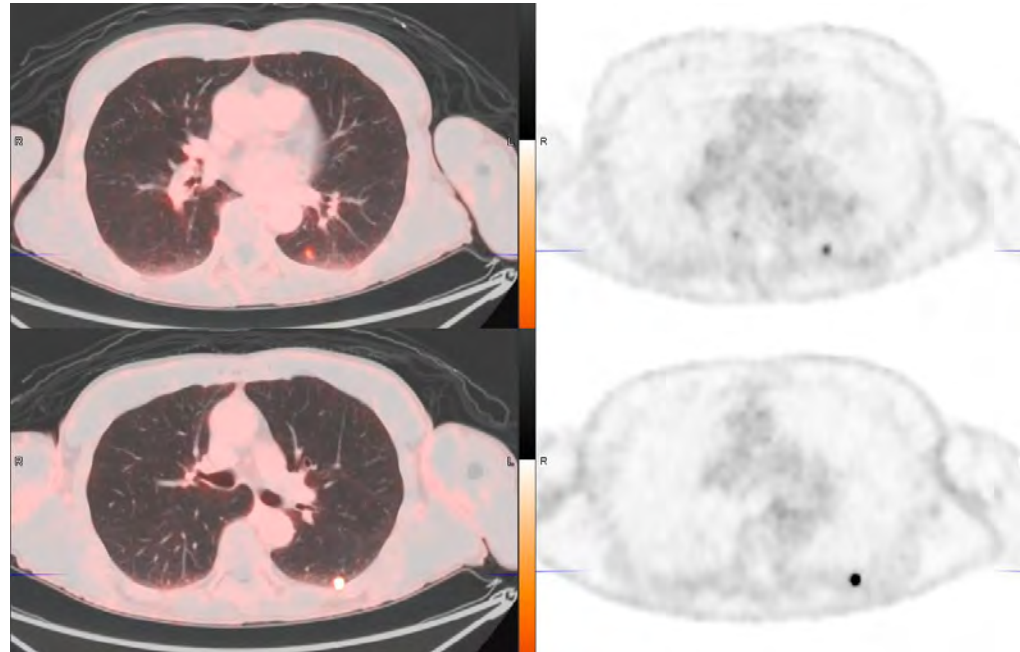
64 year-old man with BCR PC (PSA 2.88). ^{18}F -DCFPyL PET shows left supraclavicular and retroperitoneal nodal metastases.

Click on
image for
MIP video



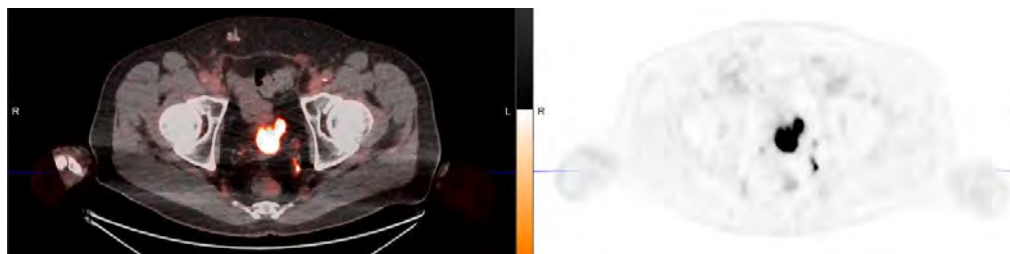
76 year-old man with BCR PC (PSA 2.6). ^{18}F -DCFPyL PET shows small retroperitoneal nodal metastases.

Click on
image
for MIP
video



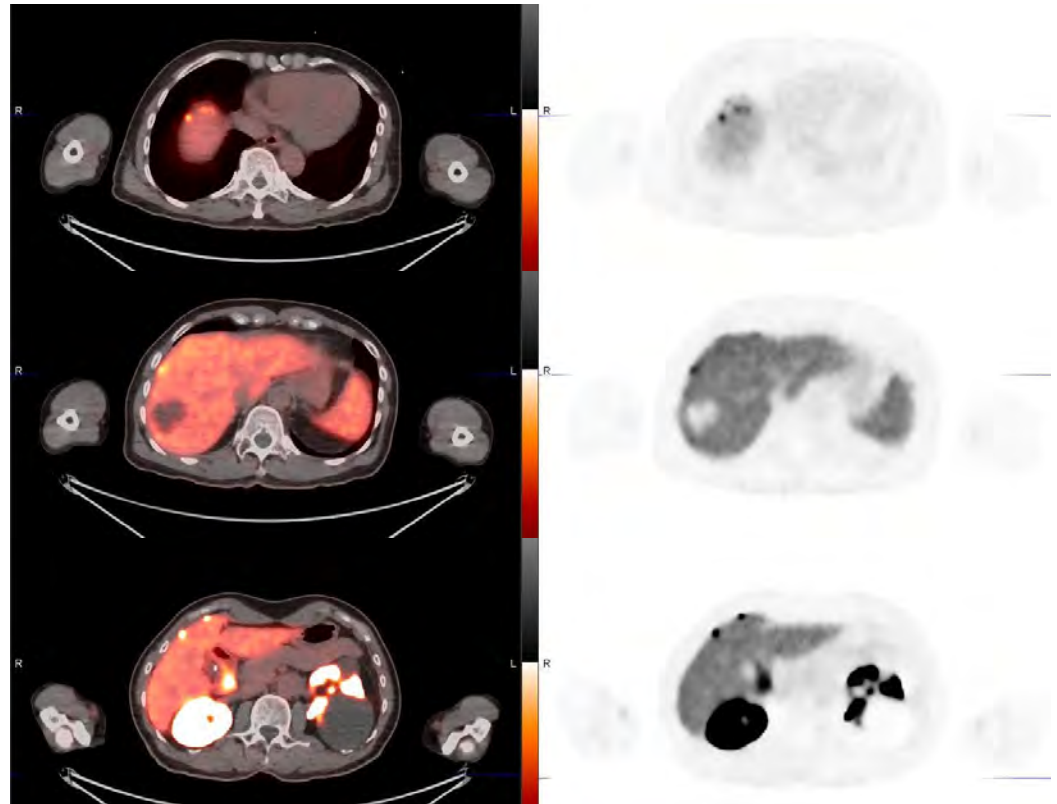
70 year-old man with BCR PC (PSA 0.69). ^{18}F -DCFPyL PET shows pulmonary metastases.

Click on
image for
MIP
video

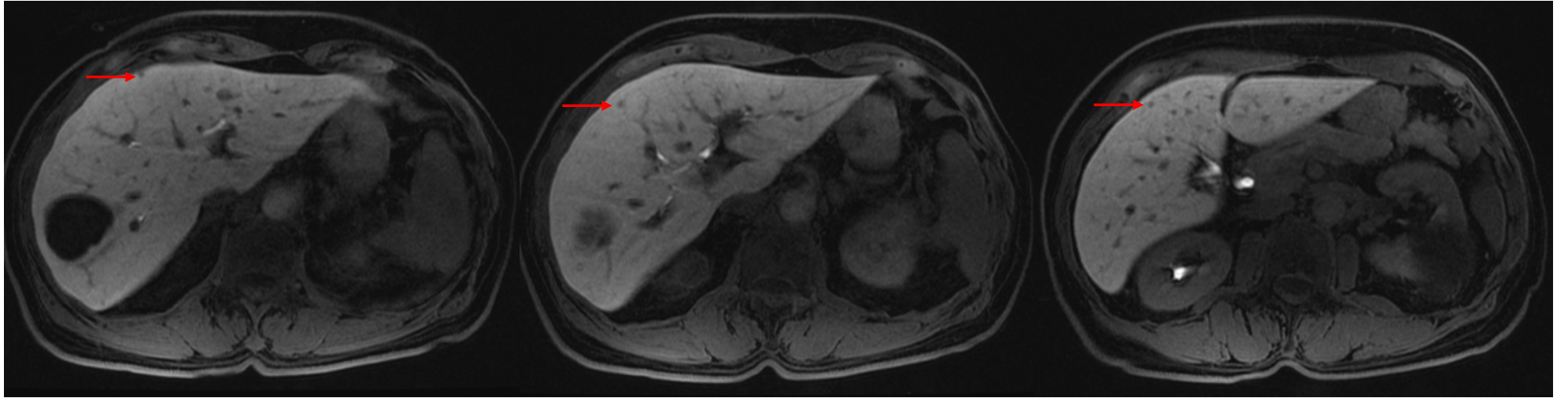


66 year-old man with BCR PC (PSA 0.5). ^{18}F -DCFPyL PET shows pelvic nodal metastasis.

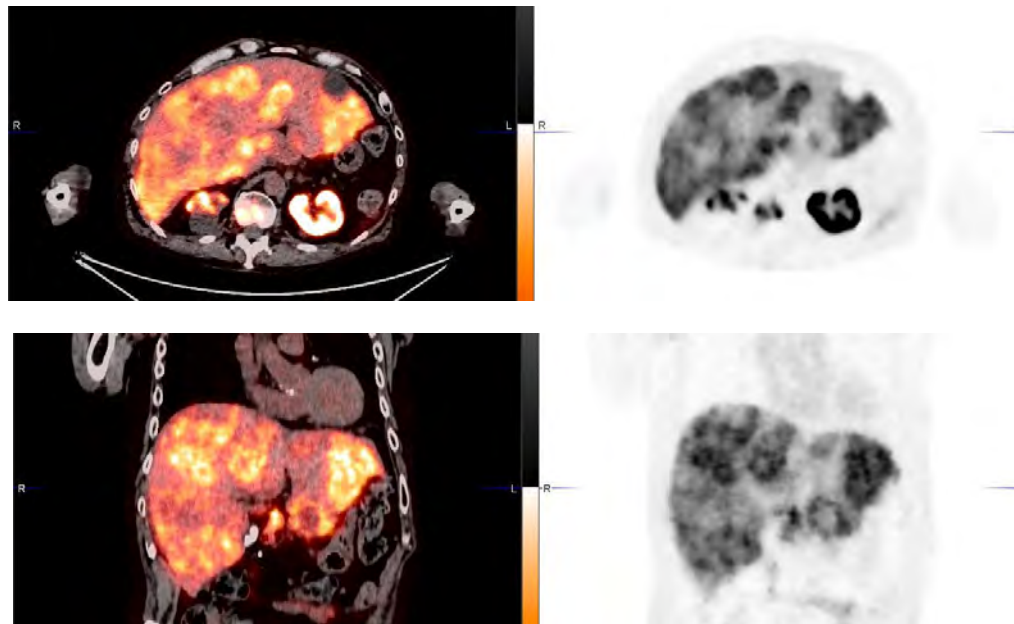
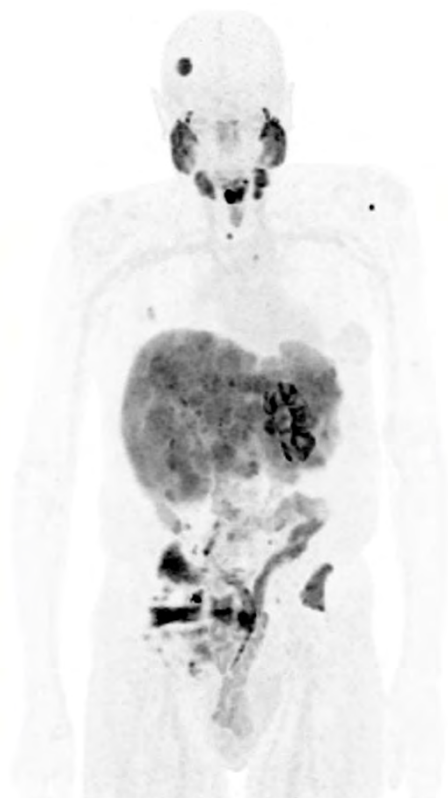
Click on
image for
MIP
video



69 year-old man with BCR PC (PSA 4.49). ^{18}F -DCFPyL PET shows nodal and liver metastases (arrows).



Click on
image for
MIP video



75 year-old man with BCR PC (PSA 698.4). ^{18}F -DCFPyL PET showed extensive hepatic, nodal and skeletal metastases.

Prospective Comparison of PET Imaging with PSMA-Targeted ^{18}F -DCFPyL Versus Na^{18}F for Bone Lesion Detection in Patients with Metastatic Prostate Cancer

Steven P. Rowe^{1,2}, Xin Li^{1,3}, Bruce J. Trock², Rudolf A. Werner^{1,4}, Sarah Frey¹, Michael DiGianvittorio^{1,5}, J. Keith Bleiler⁶, Diane K. Reyes², Rehab Abdallah¹, Kenneth J. Pienta², Michael A. Gorin^{1,2}, and Martin G. Pomper^{1,2}

THE JOURNAL OF NUCLEAR MEDICINE • Vol. 61 • No. 2 • February 2020

TABLE 1
Number of Each Type of CT Morphologic Lesion Detected by ^{18}F -DCFPyL and Na^{18}F PET

Modality	Lesion morphology on CT	Definitively positive for uptake on PET	Equivocally positive for uptake on PET	Negative for uptake on PET
^{18}F -DCFPyL PET	Sclerotic	263	4	8
	Infiltrative/marrow-based	119	0	2
	Lytic	9	0	0
Na^{18}F PET	Sclerotic	272	2	0
	Infiltrative/marrow-based	108	2	12
	Lytic	8	0	1

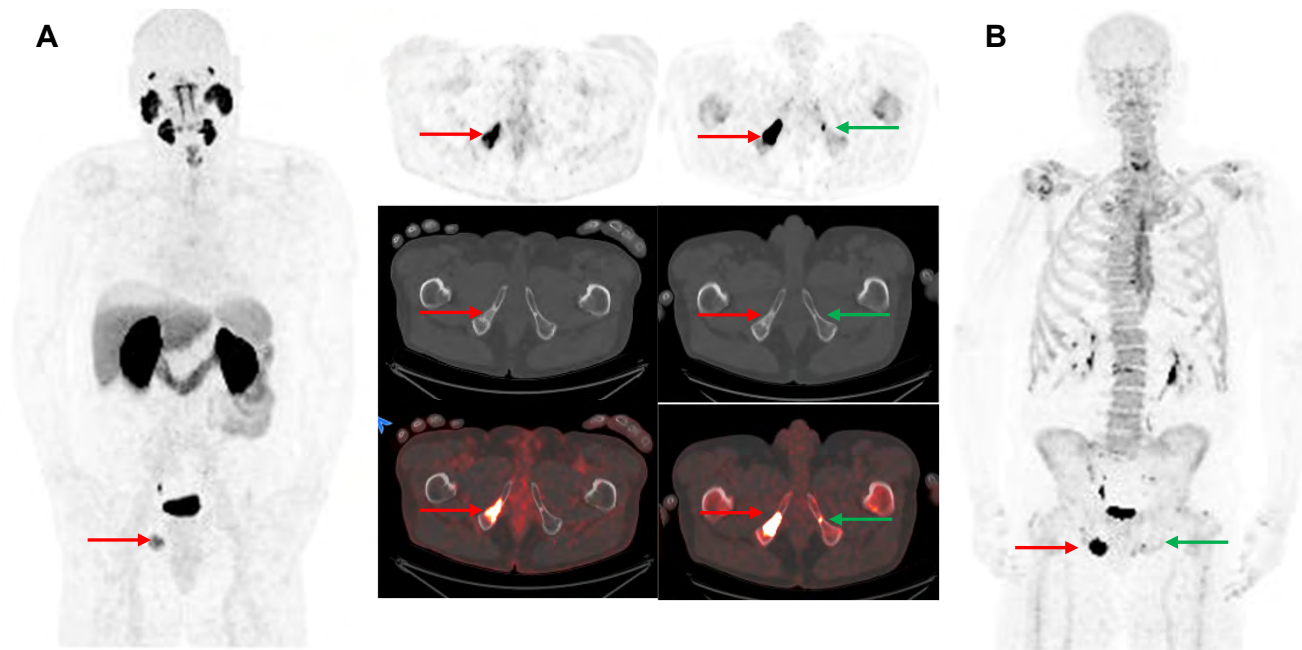
TABLE 2
Two-by-Two Table Comparing Lesion Detection Between ^{18}F -DCFPyL and Na^{18}F PET

^{18}F -DCFPyL	Na^{18}F	
	Positive	Negative
Positive	382	13
Negative	10	NA

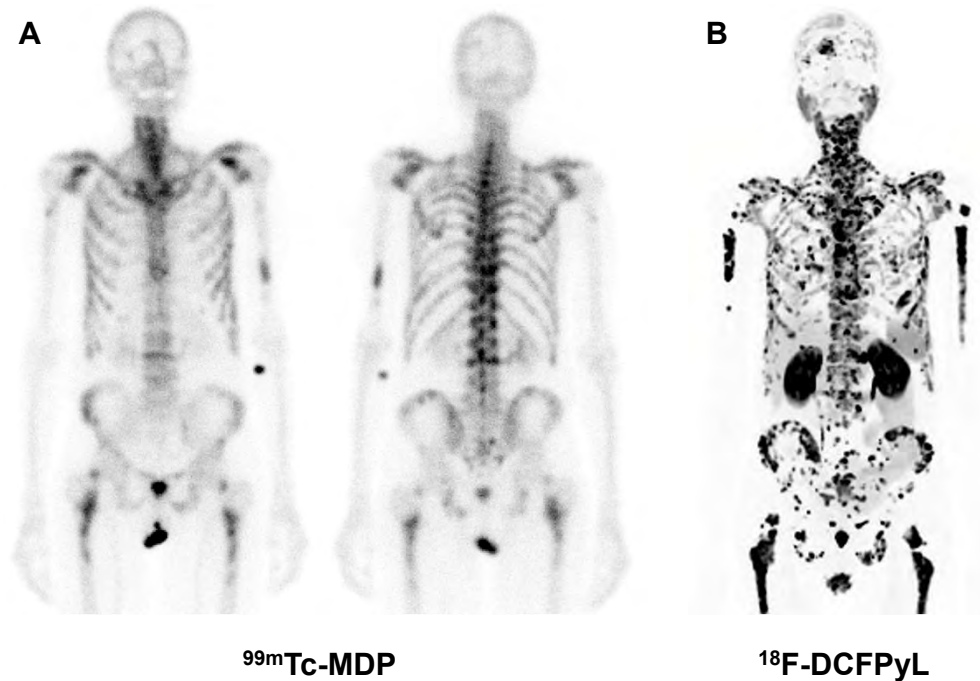
NA = not applicable.

Equivocal lesions were considered positive for this comparison.

Click on
images for
MIP video



70 year-old man with BCR PC (PSA 16.7). ^{18}F -DCFPyL PET MIP (A) and ^{18}F -NaF PET MIP (B) show uptake in a right inferior pubic ramus metastasis (red arrows). However, a small lesion in the left inferior pubic ramus is only seen on ^{18}F -NaF PET (green arrow).



[Click on
image for
MIP video](#)

74 year-old man with BCR PC (PSA 18.3) had a bone scan (A) that showed metastatic disease, but ^{18}F -DCFPyL PET MIP (B) done 1 day apart showed much more extensive skeletal metastases.

Pearls and Pitfalls

Society of Nuclear Medicine and Molecular Imaging

Patterns of uptake of prostate-specific membrane antigen (PSMA)-targeted ^{18}F -DCFPyL in peripheral ganglia

Rudolf A. Werner^{1,2} · Sara Sheikhabaie¹ · Krystyna M. Jones¹ · Mehrbod S. Javadi¹ · Lilja B. Solnes¹ · Ashley E. Ross³ · Mohamad E. Allaf⁴ · Kenneth J. Pienta⁴ · Constantin Lapa² · Andreas K. Buck² · Takahiro Higuchi^{2,5} · Martin G. Pomper¹ · Michael A. Gorin^{1,4} · Steven P. Rowe^{1,4}

Ann Nucl Med (2017) 31:696–702

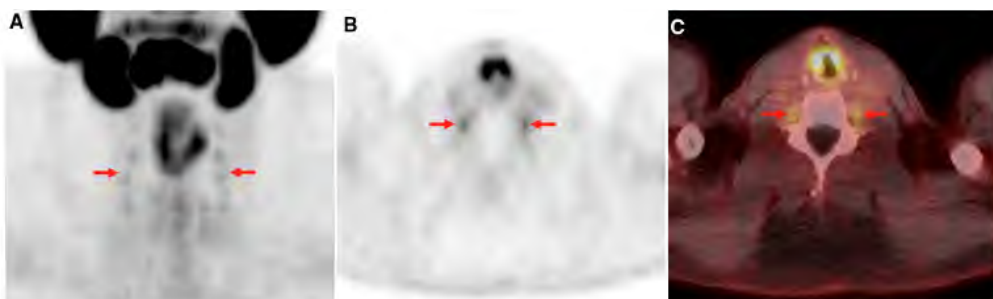


Fig. 1 a Anterior view of ^{18}F -DCFPyL maximum intensity projection (MIP) image from a 56-year-old PCA patient undergoing preoperative staging. Mild radiotracer uptake is seen in multiple cervical DRG bilaterally (*red arrows*). b Axial ^{18}F -DCFPyL PET and

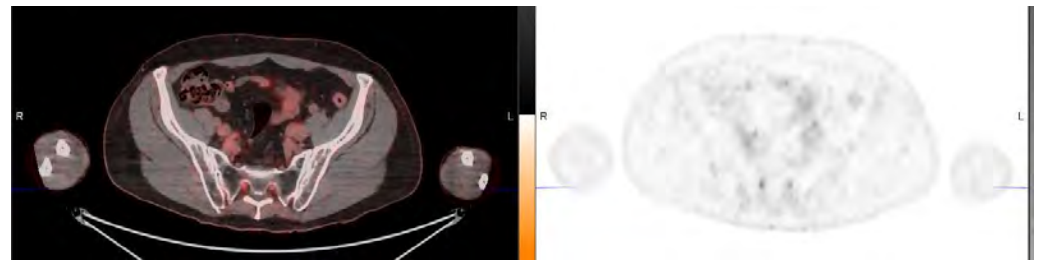
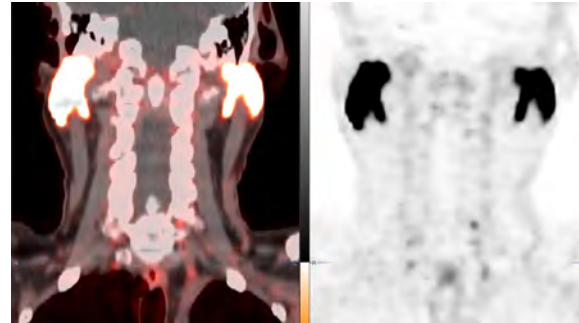
c axial ^{18}F -DCFPyL PET/CT fusion images from the C5–6 level also show mild radiotracer uptake in the C6 DRG bilaterally (*red arrows*). Note normal physiologic biodistribution of this radiotracer including uptake in the major salivary glands and structures of the larynx



Fig. 2 a Sagittal view of ^{18}F -DCFPyL MIP image from a 58-year-old female patient with history of metastatic RCC and undergoing a staging examination. Multiple lumbar and sacral DRG show mild uptake (*red arrows*). b Axial ^{18}F -DCFPyL PET and c axial ^{18}F -

DCFPyL PET/CT through the S1–2 level both demonstrate mild uptake of the S1 DRG (*red arrows*). Again, a portion of the normal physiologic biodistribution of the radiotracer is apparent including uptake in the patient's remaining kidney, liver, and bowel

Click on
image for
MIP video



62 year-old man with BCR PC (PSA 0.23). Focal uptake in peripheral ganglia is noted.

Original Article

Solitary rib lesions showing prostate-specific membrane antigen (PSMA) uptake in pre-treatment staging ⁶⁸Ga-PSMA-11 positron emission tomography scans for men with prostate cancer: benign or malignant?

Michael Y. Chen^{1,2}, Anthony Franklin^{1,2}, John Yaxley^{1,2}, Troy Gianduzzo^{1,2}, Rhiannon McBean¹, David Wong¹, Annaleis Tatkovic¹, Louise McEwan¹, James Walters¹ and Boon Kua¹

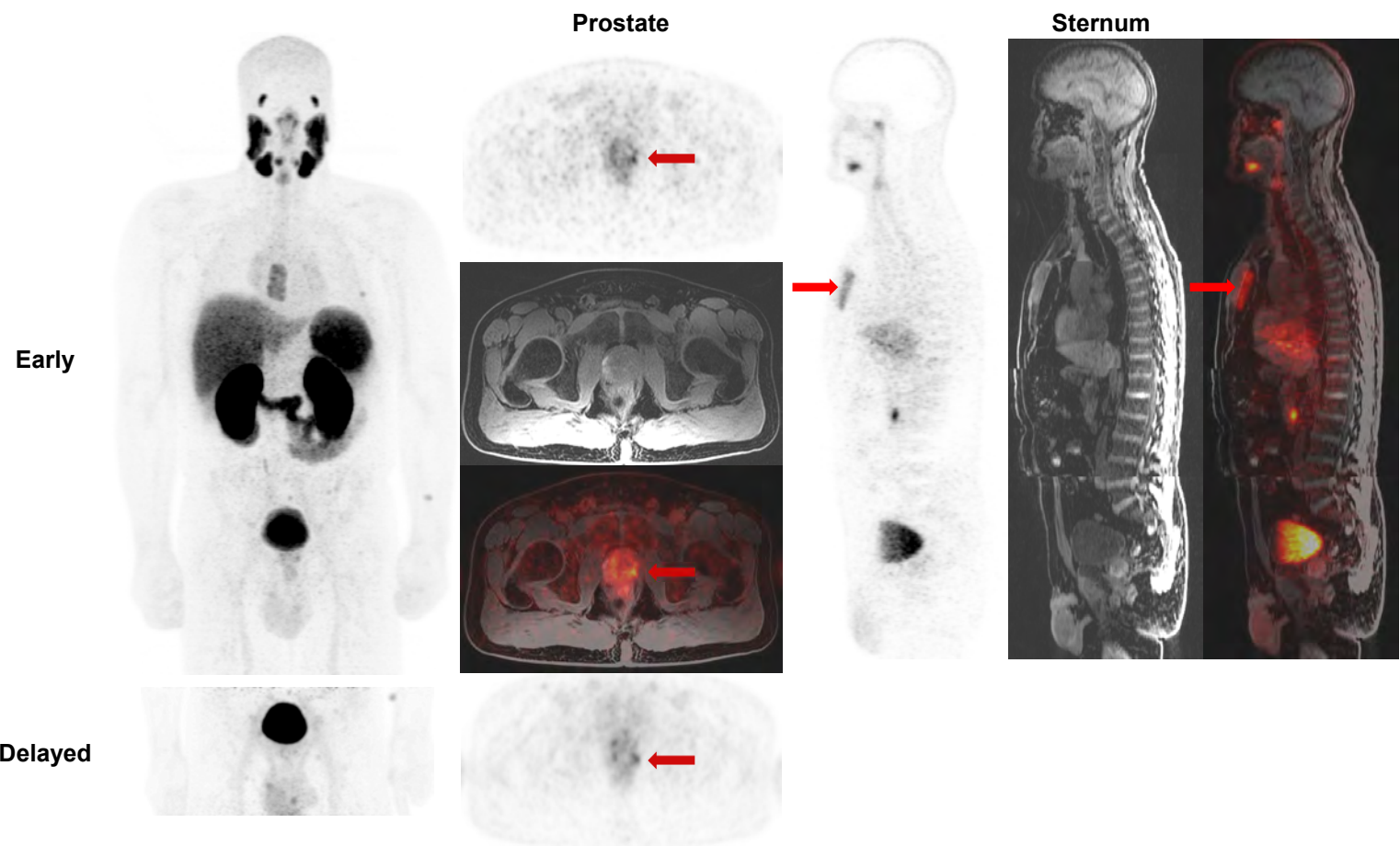
Table 2 Comparison between benign and malignant solitary rib lesions on ⁶⁸Ga-PSMA PET/CT scans.

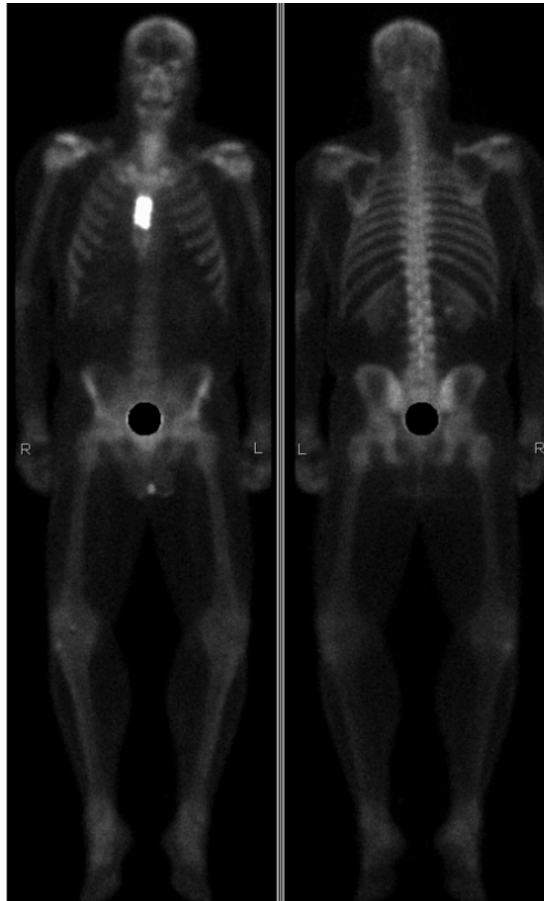
Variable	Benign	Malignant
N (%)	61 (98.4)	1 (1.6)
Age, years, median (IQR)	68 (64–72)	60
SUV _{max} , mean (SD)	3.02 (1.48)	2.21
PSA level, µg/L, mean (SD)	10.09 (10.89)	8.8
Gleason score, median (IQR)	7 (7–7)	9

IQR, interquartile range.

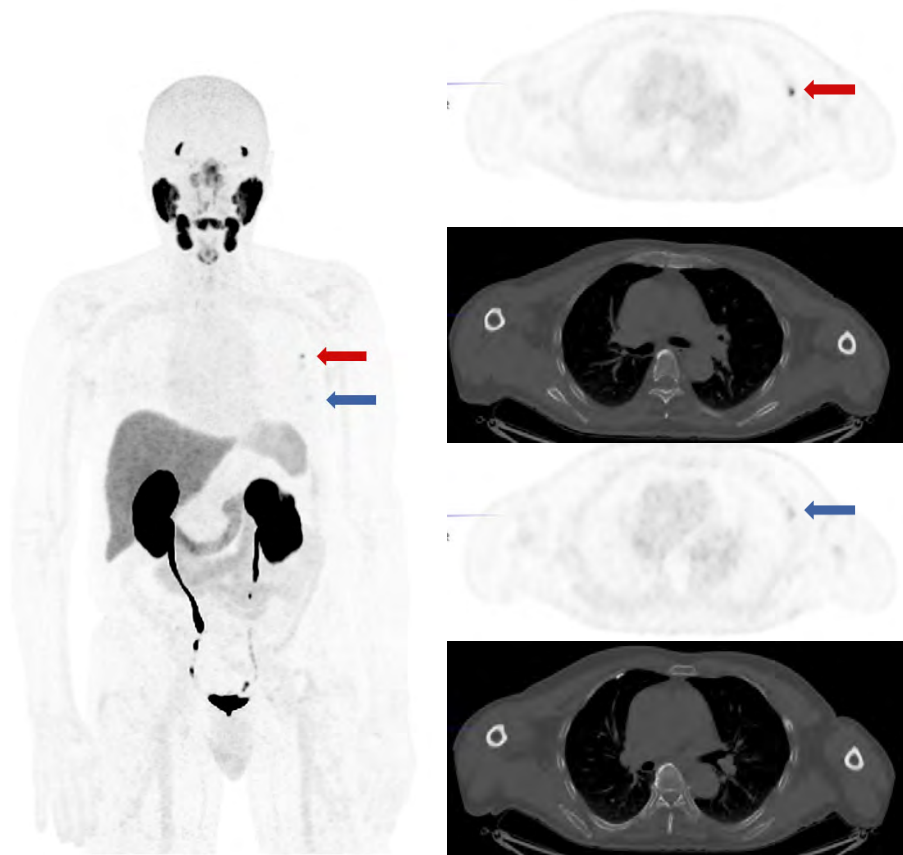
Excluding men from potentially curative local treatment based on a suspicion of solitary PSMA PET rib metastasis is not justified

*Content courtesy of Dr. Jeremie Calais.

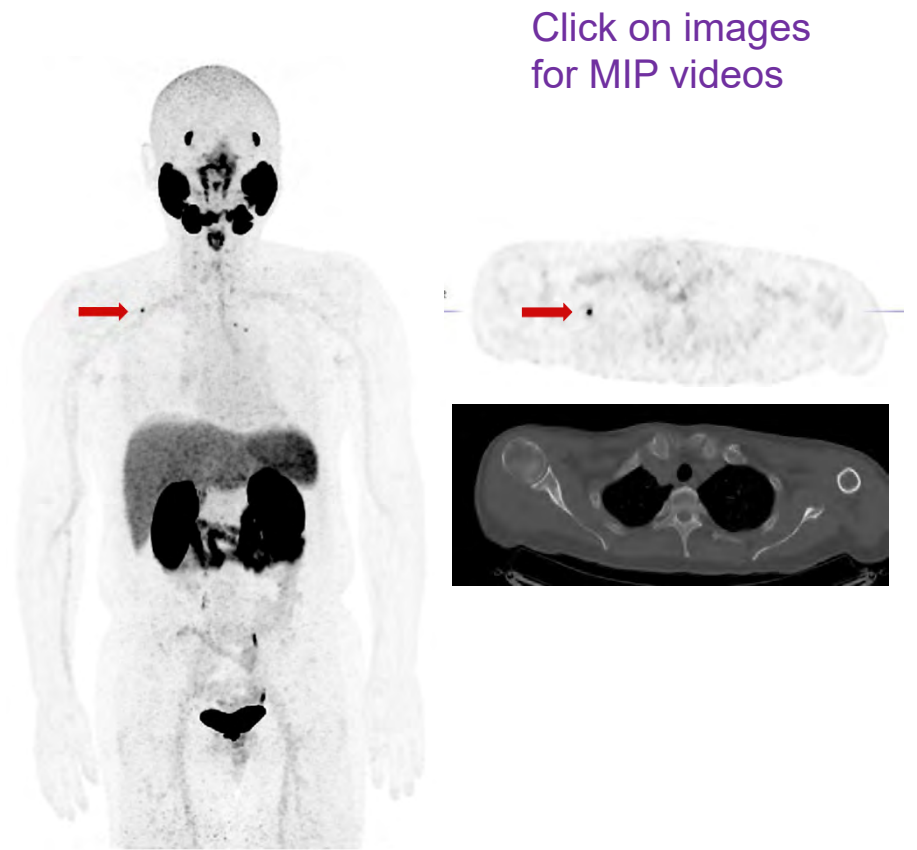




Sternal uptake is due to trauma from recent water-skiing accident.

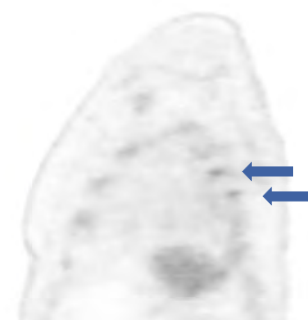
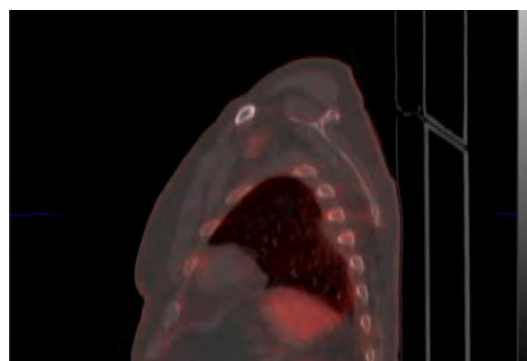


62 year-old man with BCR PC (PSA 4.07).
PSA decreased to undetectable after
radiation to the rib and pelvic LNs.



52 year-old man with BCR PC (PSA 0.176).
Solitary rib metastasis is identified.

Click on
image for
MIP video



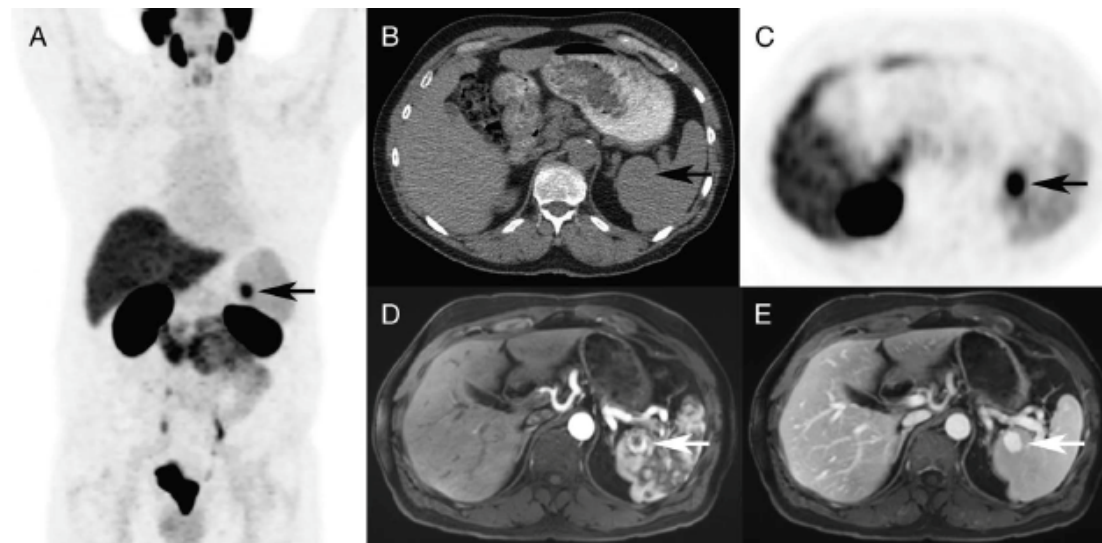
76 year-old man with BCR PC (PSA 0.47).
Low level uptake is seen in rib fractures.

Society of Nuclear Medicine and Molecular Imaging

Splenic Hemangioma as a Potential Pitfall on PSMA-Targeted ^{18}F -DCFPyL PET/CT

Guillaume Chaussé, MD, Jerome Laufer, MD, Gad Abikhzer, MD, and Stephan Probst, MD

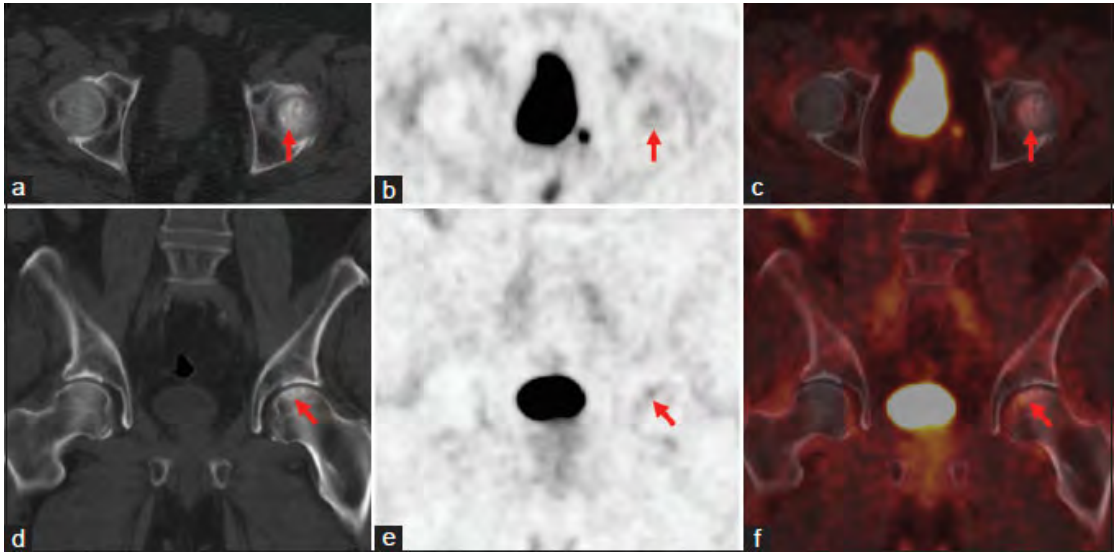
Clinical Nuclear Medicine • Volume 44, Number 3, March 2019



GONZALO TORGA¹, YAFU YIN^{1,2,3},
MARTIN G. POMPER^{1,4}, KENNETH J. PIENTA¹,
MICHAEL A. GORIN^{1,4}, STEVEN P. ROWE^{1,4}

Uptake of prostate-specific membrane antigen-targeted ¹⁸F-DCFPyL in avascular necrosis of the femoral head

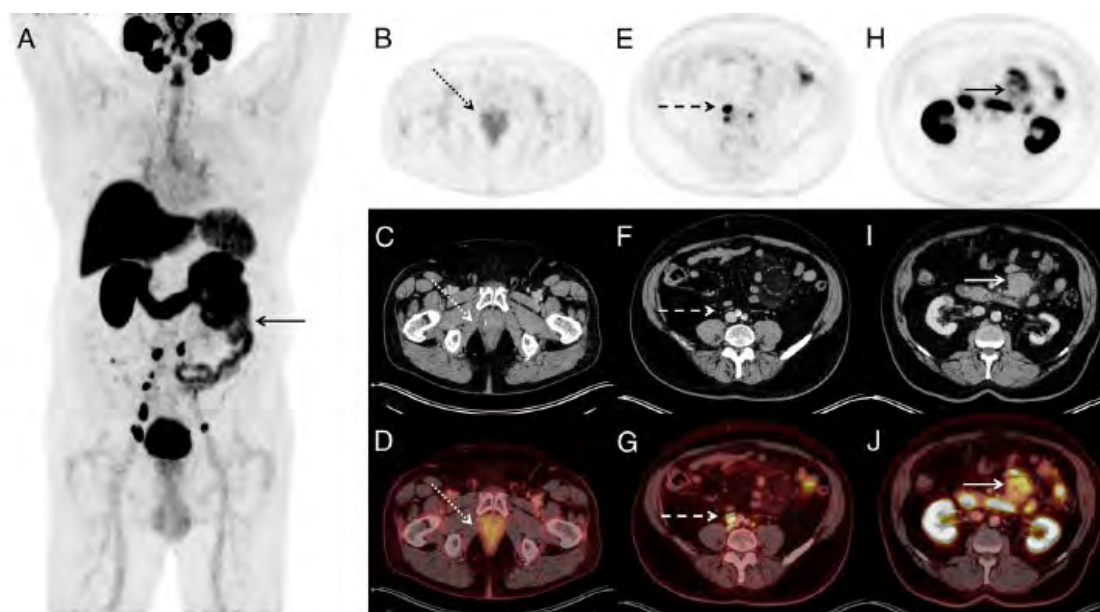
World Journal of Nuclear Medicine / Volume 18 / Issue 4 / October-December 2019



^{18}F -DCFPyL Uptake in an Incidentally Detected Follicular Lymphoma by PET/CT Performed for Biochemically Recurrent Prostate Cancer

Dennie Meijer, BSc, Maurits Wondergem, MD, PhD,† Remco J.J. Knol, MD, PhD,†
Wouter A.M. Broos, MD,† and Friso M. van der Zant, MD, PhD†*

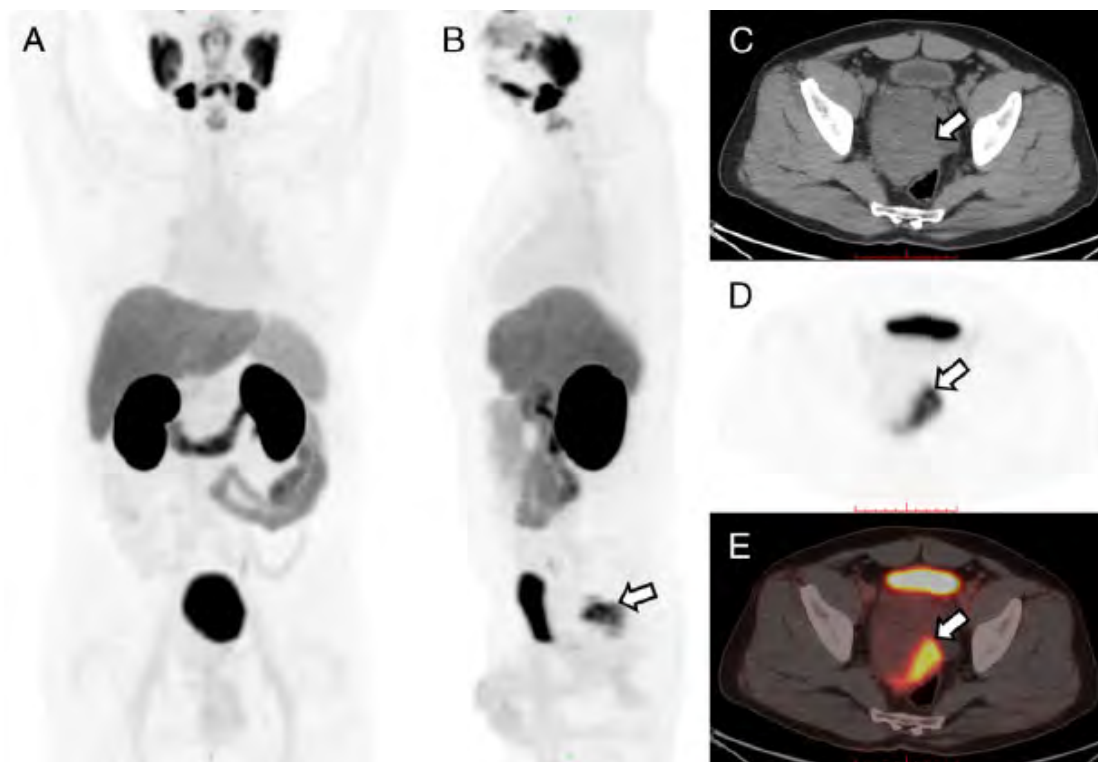
Clinical Nuclear Medicine • Volume 45, Number 2, February 2020




Primary Peripheral Primitive Neuroectodermal Tumor of the Prostate on ^{18}F -DCFPyL PET/CT

Yachao Liu, MD, and Baixuan Xu, MD

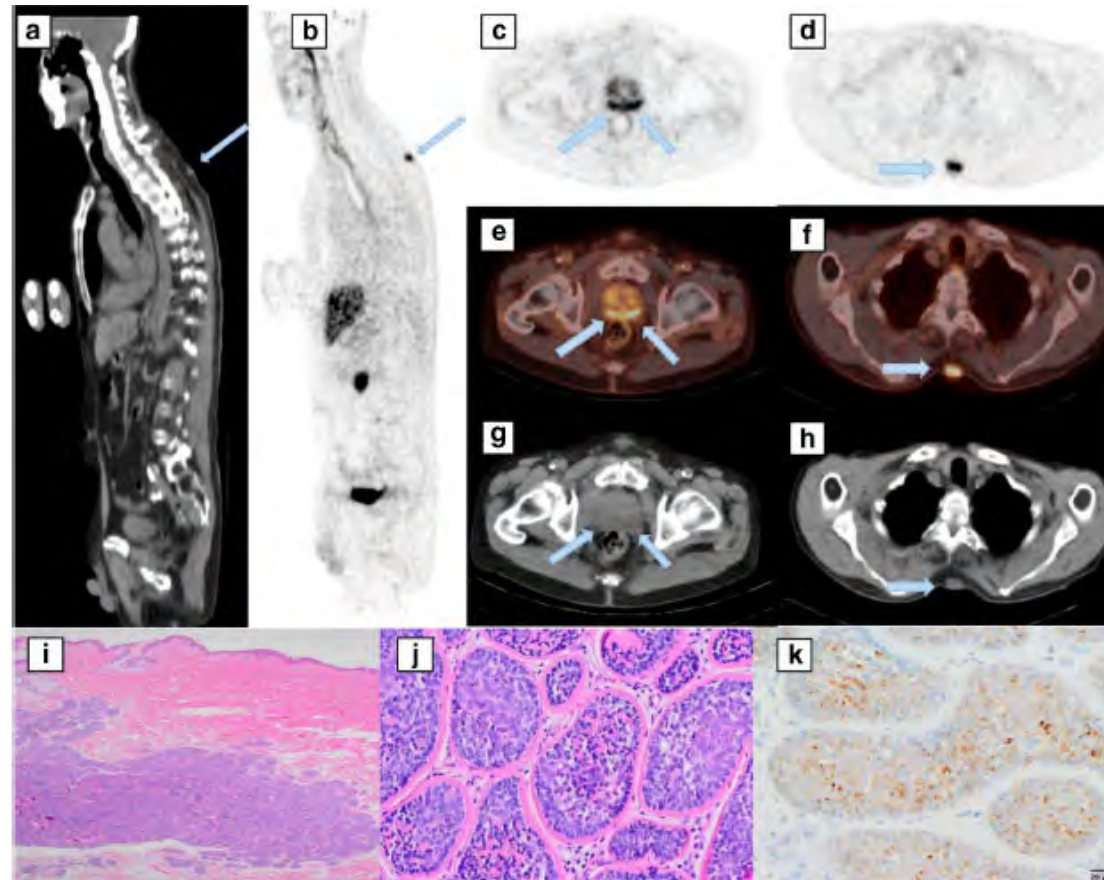
Clinical Nuclear Medicine • Volume 45, Number 5, May 2020



Cylindroma, an uncommon presentation on ^{18}F -DCFPyL PET/CT


B. P. F. Koene¹  • Y. J. L. Bodar^{1,2,3} • D. Meijer^{1,2,3} • E. H. Jaspars⁴ • A. N. Vis^{1,3} • D. E. Oprea-Lager²

European Journal of Nuclear Medicine and Molecular Imaging
<https://doi.org/10.1007/s00259-020-04943-3>

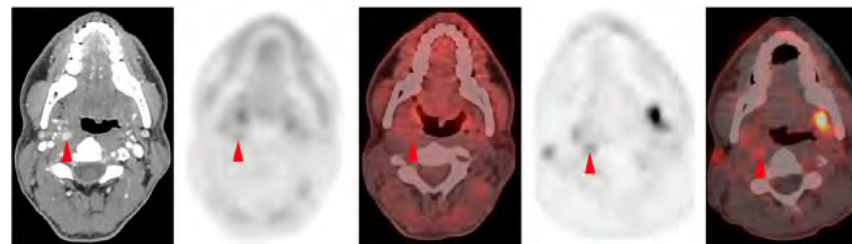


Society of Nuclear Medicine and Molecular Imaging

The prostate-specific membrane antigen (PSMA)-targeted radiotracer ^{18}F -DCFPyL detects tumor neovasculature in metastatic, advanced, radioiodine-refractory, differentiated thyroid cancer

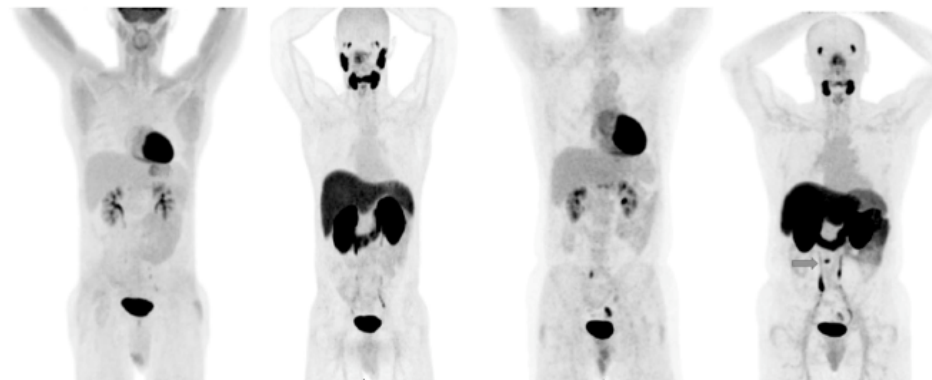
Prasanna Santhanam^{1,5}  · Jonathon Russell² · Lisa M. Rooper³ · Paul W. Ladenson¹ · Martin G. Pomper⁴ · Steven P. Rowe⁴

Medical Oncology (2020) 37:98



Patient 1

Patient 2



FDG PET/CT

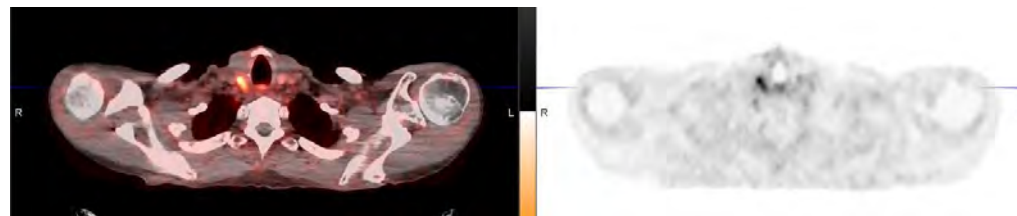
DCFPyL PET/CT

FDG PET/CT

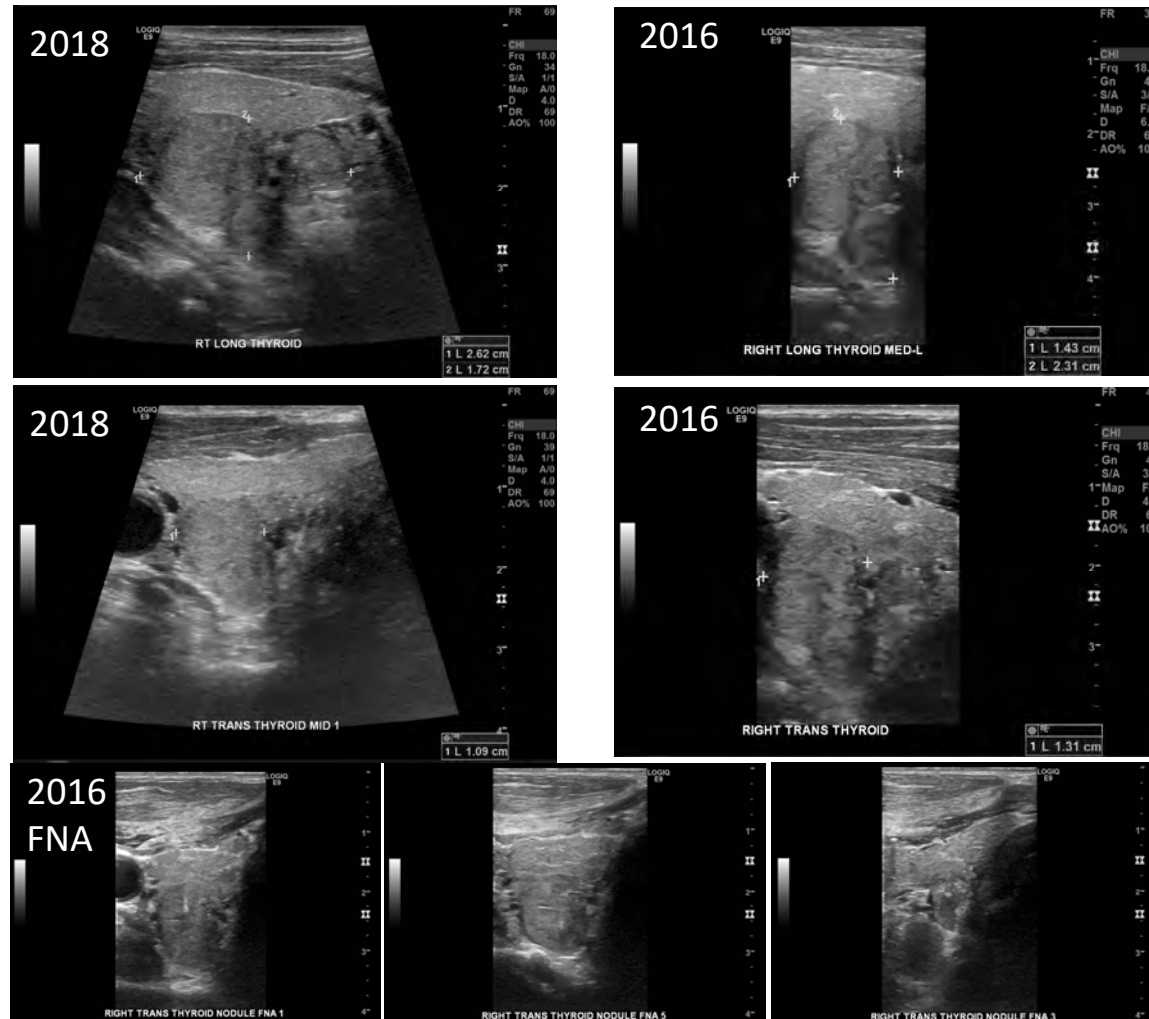
DCFPyL PET/CT

Society of Nuclear Medicine and Molecular Imaging

Click on
image for
MIP video



76 year-old man with BCR PC (PSA 18). Focal uptake is seen in the thyroid.



Nodule was biopsied
and pathology report
indicated adenoma.

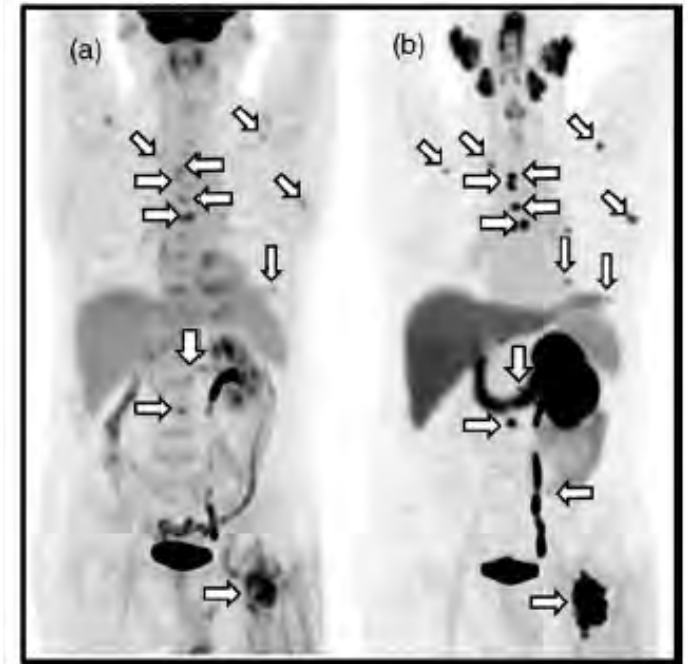
Comparison of ^{18}F -DCFPyL and ^{18}F -FDG PET/computed tomography for the restaging of clear cell renal cell carcinoma: preliminary results of 15 patients

Yachao Liu^{a,*}, Guanyun Wang^{a,b,*}, Hongkai Yu^c, Yue Wu^d, Mu Lin^d, Jiangping Gao^c and Baixuan Xu^a

Nuclear Medicine Communications 2020, 41:1299–1305



Representative transaxial computed tomography (CT) image (a), fused ^{18}F -FDG PET/CT image (b), and fused ^{18}F -DCFPyL PET/CT image (c) in Patient no. 5. One lesion was found around the postoperative left kidney (white arrow). This lesion was diagnosed as a recurrent focus of clear cell renal cell carcinoma (ccRCC) by postoperative pathology. ^{18}F -DCFPyL PET/CT, ^{18}F -labeled low-molecular weight PSMA ligand 2-(3-(1-carboxy-5-[(6-[^{18}F]fluoropyridine-3-carbonyl)-amino]-pentyl)-ureido)-pentanedioic acid; ^{18}F -FDG, 2-deoxy-2-[^{18}F]fluoro-D-glucose.



Representative transaxial computed tomography (CT) image, (a) fused ^{18}F -FDG PET/CT image (b), and fused ^{18}F -DCFPyL PET/CT image (c) in Patient no. 14. One lesion was found in the right renal fossa (white arrow). This lesion was eventually diagnosed as a postoperative change by follow-up. ^{18}F -DCFPyL PET/CT, ^{18}F -labeled low-molecular weight PSMA ligand 2-(3-(1-carboxy-5-[(6-[^{18}F]fluoropyridine-3-carbonyl)-amino]-pentyl)-ureido)-pentanedioic acid; ^{18}F -FDG, 2-deoxy-2-[^{18}F]fluoro-D-glucose.

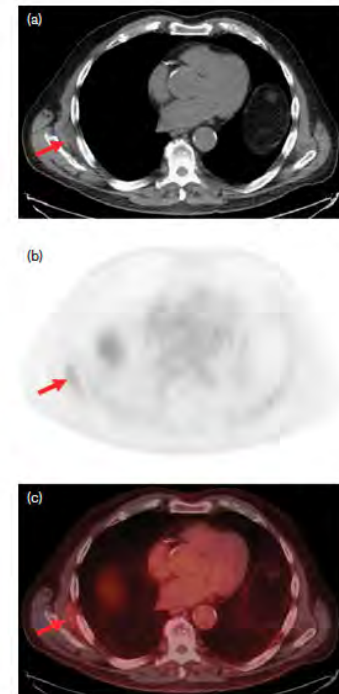
Uptake of the prostate-specific membrane antigen-targeted PET radiotracer ^{18}F -DCFPyL in elastofibroma dorsi

Michael A. Gorin^a, Wael Marashdeh^b, Ashley E. Ross^a, Mohammad E. Allaf^a,
Kenneth J. Pienta^a, Martin G. Pomper^b and Steven P. Rowe^b

Nuclear Medicine Communications 2017, **38**:795–798



Bilateral elastofibroma dorsi (red arrows) demonstrating uptake of the ^{18}F -DCFPyL radiotracer. Axial (a) noncontrast computed tomography (CT), (b) PET, and (c) fused PET/CT images.



Right-sided elastofibroma dorsi (red arrow) demonstrating uptake of the ^{18}F -DCFPyL radiotracer. Axial (a) noncontrast computed tomography (CT), (b) PET, and (c) fused PET/CT images.


Pearls and pitfalls in clinical interpretation of prostate-specific membrane antigen (PSMA)-targeted PET imaging

Sara Sheikhabaei¹ • Ali Afshar-Oromieh² • Matthias Eiber^{3,4} • Lilja B. Solnes¹ • Mehrbod S. Javadi¹ • Ashley E. Ross⁵ • Kenneth J. Pienta⁵ • Mohamad E. Allaf⁵ • Uwe Haberkorn² • Martin G. Pomper¹ • Michael A. Gorin⁵ • Steven P. Rowe¹

Eur J Nucl Med Mol Imaging (2017) 44:2117–2136

*Michael S. Hofman, MBBS, FRACP,
FAANMS
Rodney J. Hicks, MD, MBBS, FRACP
Tobias Maurer, MD
Matthias Eiber, MD²*

RadioGraphics 2018; 38:200–217

 **Prostate-specific Membrane
Antigen PET: Clinical Utility in
Prostate Cancer, Normal Patterns,
Pearls, and Pitfalls¹**

Reporting ^{18}F DCFPyL PET

About the report

- The report describes the performance of the test
- The report interprets the test
- The report reflects on the author(s), the department and the medical center
- The report is a permanent record and should be crafted so that it is a pleasure to read after days, weeks, months or years
- The report is a medical legal document

Report content

- Identification
- Indication/Clinical history (relevant)
- Comparison/Correlating studies
- Procedure
 - ✓ Radiopharmaceutical
 - ✓ Administered activity
 - ✓ Route
 - ✓ Protocol
- Findings
- Impression

Findings and Interpretation

- Avoid describing everything seen but not giving an interpretation
- Avoid rambling description of findings without a reasonable conclusion
- Avoid language that pushes referring MD into inaction
- ACR Standard for Communication in “Standards 2002-2003”:
“Precise diagnosis...wherever possible. Differential diagnosis when appropriate and follow-up or additional studies when appropriate”

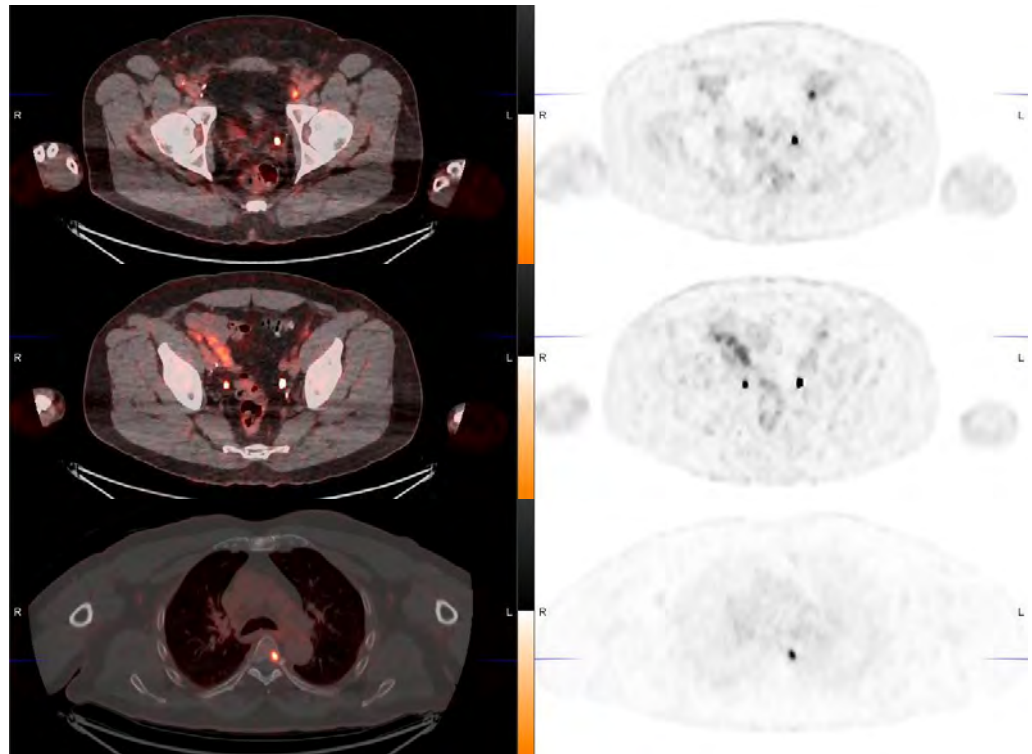
Findings and Interpretation

- This is often all that is read
- Start with statement normal or abnormal
- Answer the clinical question asked by referring physician

Good Reports are:

- Clear
- Concise (brief)
- Complete
- Consistent
- Clinically relevant
- Communication (documented)

Click on
image
for MIP
video



64 year-old man with BCR PC (0.3). ^{18}F -DCFPyL PET showed nodal and skeletal metastases.

Sample ^{18}F -DCFPyL report

F18- DCFPyL PET/CT: mo/day/year time

CLINICAL HISTORY: xy years of age, Male, with history of prostate cancer s/p robotic prostatectomy and negative bilateral pelvic lymph node dissection. He is being considered for salvage radiotherapy in the setting of rising PSA (0.3). He is referred for evaluation of recurrent or metastatic disease. This PET/CT scan is requested for restaging.

PET SEQUENCE: Subsequent treatment strategy

COMPARISON: None.

PROCEDURE COMMENTS:

Tracer information:

Measured (injected) dose: 9.0 mCi of F18-DCFPyL.

Injection site: Right forearm.

Anatomical region: The area imaged included the skull base to mid thighs

Scan technique: Following IV administration of the radiopharmaceutical, images were acquired using a MI PET-CT scanner. A low-dose CT scan was performed for attenuation correction and anatomic correlation only. If a comprehensive diagnostic CT is required, the Department of Radiology should be consulted for an adjunct CT study. Images were reconstructed using OSEM or BSREM algorithms. CTAC dose information: Based on a 32 cm phantom, the estimated radiation dose (CTDIvol [mGy]) for each series in this exam is 3.89. The estimated cumulative dose (DLP [mGy-cm]) is 441.31.

Images were reviewed in the axial, coronal, and sagittal planes. For descriptive purposes, the maximum standard uptake value (SUV max) of radiotracer-avid tissues is reported in g/mL, unless stated otherwise. The image number corresponding to the CT series is provided in reference to findings.

Sample ^{18}F -DCFPyL report, cont.

FINDINGS:

F18 DCFPyL PET: Physiologic distribution of tracer is seen salivary and lacrimal glands, blood pool, liver, spleen, pancreas, ganglia, bone marrow, bowel, kidneys and urinary tract.

Evaluation of the prostate bed: There is no focal PyL uptake in the prostate bed to suggest local recurrence.

Evaluation of lymph nodes: There are multiple sites of focal PyL uptake in lymph nodes compatible with nodal metastases. They involve pelvic and retroperitoneal lymph nodes:

- * Image 273, left presacral node, 4 x 4 mm
- * Image 272, right pelvic sidewall node just anterior to the ureter, 6 x 3 mm
- * Image 298, left obturator node, 12 x 11 mm
- * Image 25, right external iliac node, 9 x 7 mm
- * Image 252, left common iliac, 5 x 3 mm

Evaluation of skeleton: There is focal PyL uptake in the skeleton compatible with osseous metastases:

- * Image 160, right pedicle of T8 with SUV 4.2
- * Image 135, the left posterior aspect of T5, SUV 14.3

Incidental CT: Lung parenchymal evaluation, including for punctate nodules, is limited by low-dose CT and non-breathhold technique. There is a nonspecific 3 mm nodule in the right middle lobe in image 162.

IMPRESSION:

1. PyL binding in the spine and pelvic and retroperitoneal lymph nodes compatible with metastatic prostate malignancy.

⁶⁸Ga-PSMA PET/CT: Joint EANM and SNMMI procedure guideline for prostate cancer imaging: version 1.0

Wolfgang P. Fendler^{1,2} • Matthias Eiber^{1,3} • Mohsen Beheshti⁴ • Jamshed Bomanji⁵ • Francesco Ceci⁶ • Steven Cho⁷ • Frederik Giesel⁸ • Uwe Haberkorn⁸ • Thomas A. Hope⁹ • Klaus Kopka¹⁰ • Bernd J. Krause¹¹ • Felix M. Mottaghy^{12,13} • Heiko Schöder¹⁴ • John Sunderland¹⁵ • Simon Wan⁵ • Hans-Jürgen Wester¹⁶ • Stefano Fanti⁶ • Ken Herrmann^{1,17}

Published online: 10 March 2017
© Springer-Verlag Berlin Heidelberg 2017


Prostate Cancer Molecular Imaging Standardized Evaluation (PROMISE): Proposed miTNM Classification for the Interpretation of PSMA-Ligand PET/CT

Matthias Eiber^{1,2}, Ken Herrmann^{1,3}, Jeremie Calais¹, Boris Hadaschik⁴, Frederik L. Giesel⁵, Markus Hartenbach⁶, Thomas Hope⁷, Robert Reiter⁸, Tobias Maurer⁹, Wolfgang A. Weber¹⁰, and Wolfgang P. Fendler^{1,11}

PSMA-RADS Version 1.0: A Step Towards Standardizing the Interpretation and Reporting of PSMA-targeted PET Imaging Studies

Steven P. Rowe^{a,b,*}, Kenneth J. Pienta^b, Martin G. Pomper^{a,b}, Michael A. Gorin^{a,b}

Development of standardized image interpretation for ⁶⁸Ga-PSMA PET/CT to detect prostate cancer recurrent lesions

Stefano Fanti¹ • Silvia Minozzi² • Joshua James Morigi³  • Frederik Giesel⁴ • Francesco Ceci¹ • Christian Uprimny⁵ • Michael S. Hofman⁶ • Matthias Eiber⁷ • Sarah Schwarzenbock⁸ • Paolo Castellucci¹ • Cristina Bellisario⁹ • Stéphane Chauvie¹⁰ • Fabrizio Bergesio¹⁰ • Louise Emmett³ • Uwe Haberkorn⁴ • Irene Virgolini⁵ • Markus Schwaiger⁷ • Rodney J. Hicks⁶ • Bernd J. Krause⁸ • Arturo Chiti¹¹



Comparison of three interpretation criteria of ^{68}Ga -PSMA11 PET based on inter- and intra-reader agreement

Akira Toriihara, Tomomi Nobashi, Lucia Baratto, Heying Duan, Farshad Moradi, Sonya Park, Negin Hatami, Carina Aparici, Guido Davidzon and Andrei Iagaru

J Nucl Med.

Published online: September 27, 2019.

Doi: 10.2967/jnumed.119.232504

Table 4: Inter-reader agreement of each interpretation criteria (Gwet's AC)

Site	EANM	PROMISE	PSMA-RADS
<Group 1 (PET/MRI for initial staging)>			
Local sites	0.70	0.75	0.73
Lymph node metastases	0.93	0.93	0.93
Distant metastases	0.96	0.97	0.89
Final judgement	0.89	0.79	0.72
<Group 2 (PET/CT due to biochemical recurrence)>			
Local sites	0.69	0.73	0.77
Lymph node metastases	0.80	0.79	0.78
Distant metastases	0.84	0.80	0.57
Final judgement	0.79	0.67	0.64

*Moderate agreement

Notes: CT, computed tomography; EANM, European Association of Nuclear Medicine; MRI, magnetic resonance imaging; PET, positron emission tomography; PROMISE, prostate cancer molecular imaging standardized evaluation; PSMA, prostate-specific membrane antigen; PSMA-RADS, PSMA-reporting and data system

Table 5: Intra-reader agreement of each interpretation criteria (Gwet's AC)

Site	EANM	PROMISE	PSMA-RADS
<Group 1 (PET/MRI for initial staging)>			
Local sites	0.95/0.63	0.93/0.74	0.98/0.70
Lymph node metastases	0.93/0.98	0.79/0.98	0.93/0.98
Distant metastases	0.93/1.00	0.96/0.98	0.98/0.98
Final judgement	0.95/0.94	0.91/0.77	0.88/0.75
<Group 2 (PET/CT due to biochemical recurrence)>			
Local sites	0.93/0.78	0.91/0.78	0.93/0.78
Lymph node metastases	0.90/0.79	0.86/0.73	0.86/0.69
Distant metastases	0.92/0.83	0.83/0.81	0.75/0.81
Final judgement	0.91/0.73	0.93/0.52	0.91/0.49

Each Gwet's AC was expressed as "reader 1/reader 2".

*Moderate agreement


Notes: CT, computed tomography; EANM, European Association of Nuclear Medicine; MRI, magnetic resonance imaging; PET, positron emission tomography; PROMISE, prostate cancer molecular imaging standardized evaluation; PSMA, prostate-specific membrane antigen; PSMA-RADS, PSMA-reporting and data system

Table 6: Inter-criteria agreement of each site

Site	Gwet's AC
<Group 1 (PET/MRI for initial staging)>	
Local	0.92
Lymph node	0.97
Distant	0.96
Final judgement	0.93
<Group 2 (PET/CT due to biochemical recurrence)>	
Local	0.97
Lymph node	0.98
Distant	0.72
Final judgement	0.91

Notes: CT, computed tomography; MRI, magnetic resonance imaging; PET, positron emission tomography

E-PSMA: the EANM standardized reporting guidelines v1.0 for PSMA-PET

Francesco Ceci¹ • Daniela E. Oprea-Lager²  • Louise Emmett^{3,4} • Judit A. Adam⁵ • Jamshed Bomanji⁶ • Johannes Czernin⁷ • Matthias Eiber⁸ • Uwe Haberkorn⁹ • Michael S. Hofman^{10,11} • Thomas A. Hope¹² • Rakesh Kumar¹³ • Steven P. Rowe¹⁴ • Sarah M. Schwarzenboeck¹⁵ • Stefano Fanti¹⁶ • Ken Hermann¹⁷

#	Open Questions for Panelists	Level of Agreement	Agreed Answer
1	Do you think PSMA standardized and structured report is necessary?	k=1.0	In favour
2	Do you agree with the inclusion of synoptic tables in the report (Synoptic Table 1 and 2), in order to provide more reproducible information?	k=1.0	In favour
3	Do you agree with the inclusion of technical information in the report (as described in Synoptic Table 1)?	k=1.0	In favour
4	Do you think that reader experience (in reading PSMA images) should be disclosed in the report?	k=1.0	Against
5	Do you agree with the proposed 5-point scale to rate the quality of the scan as reported in Synoptic Table 1? (Quality scale: 1=very poor/non-diagnostic; 2=poor; 3=moderate; 4=good; 5=excellent)	k=0.91	Against
6	Do you agree with the standard acquisition protocol (vertex to mid-thigh)?	k=1.0	In favour
7	Do you agree with the whole-body acquisition protocol (lower extremities included) in those patients eligible for radio-ligand therapy?	k=0.82	In favour
8	Do you agree with the use of miTNM (PROMISE criteria) for the anatomical identification of the lesions (region-based)?	k=1.0	In favour
9	Do you agree with the inclusion of visual PSMA expression (PSMA Expression V - Synoptic Table 2) in the report?	k=1.0	In favour
10	Do you agree with the proposed 4-point scale (0 to 3) for PSMA Expression V?	k=1.0	In favour
11	Do you agree with the inclusion of quantitative PSMA expression (PSMA Expression Q - Synoptic Table 2) in the report?	k=1.0	In favour
12	Do you agree with the use of tumor to background ratio (TBR) instead of SUVmax for PSMA Expression Q?	k=0.82	Against
13	Do you agree with the inclusion of PSMA-RADS in the report (Synoptic Table 2), as method to evaluate reader confidence?	k=0.61	Not reached
14	Do you agree with the proposed 5-point scale for PSMA-RADS?	k=0.55	Not reached
15	Do you agree with the use of sub-categories (1A and 1B - 3A, 3B, 3C, 3D) for PSMA-RADS?	k=0.73	Against
16	Do you agree with the inclusion of eventual incidental findings in the report?	k=1.0	In favour

Table 2 Qualitative evaluation of PSMA expression through a 4-point scale

PSMA expression V (visual score)	Grade of PSMA expression
Score=0	Below blood pool
Score=1	Equal to or above blood pool and lower than liver
Score=2	Equal to or above liver and lower than parotid gland
Score=3	Equal to or above parotid gland

Table 3 Regional classification of PSMA-PET findings

Class	Description
Local tumor (T)	
miT0	No local tumor
miT2	Organ-confined tumor
miT3a	Non-organ-confined tumor (extracapsular extension)
miT3b	Non-organ-confined tumor (seminal vesicles invasion)
miT4	Tumor invading adjacent structures (other than seminal vesicles)
miTr	Presence of local recurrence after radical prostatectomy
Regional nodes (N)	
miN0	No positive regional lymph nodes
miN1	Positive regional lymph nodes
Distant metastases (M)	
miM0	No distant metastases
miM1a	Extra-pelvic lymph nodes
miM1b	Bone metastasis
miM1c	Non-nodal visceral metastasis: report involved organ(s)

E-PSMA: the EANM standardized reporting guidelines v1.0 for PSMA-PET


Francesco Ceci¹ • Daniela E. Oprea-Lager²  • Louise Emmett^{3,4} • Judit A. Adam⁵ • Jamshed Bomanji⁶ • Johannes Czernin⁷ • Matthias Eiber⁸ • Uwe Haberkorn⁹ • Michael S. Hofman^{10,11} • Thomas A. Hope¹² • Rakesh Kumar¹³ • Steven P. Rowe¹⁴ • Sarah M. Schwarzenboeck¹⁵ • Stefano Fanti¹⁶ • Ken Hermann¹⁷

Table 4 Interpretation of PSMA-PET findings according to the reader confidence expressed through a 5-point scale

Score	Definition
1	Benign lesion without abnormal PSMA uptake
2	Probably benign lesion: faint PSMA uptake (equal or lower than background) in a site atypical for prostate cancer
3	Equivocal finding: faint uptake in a site typical for prostate cancer or intense uptake in a site atypical for prostate cancer
4	Probably prostate cancer: intense uptake in typical site of prostate cancer, but without definitive findings on CT*
5	Definitive evidence of prostate cancer: intense uptake in typical site of prostate cancer, with definitive findings on CT

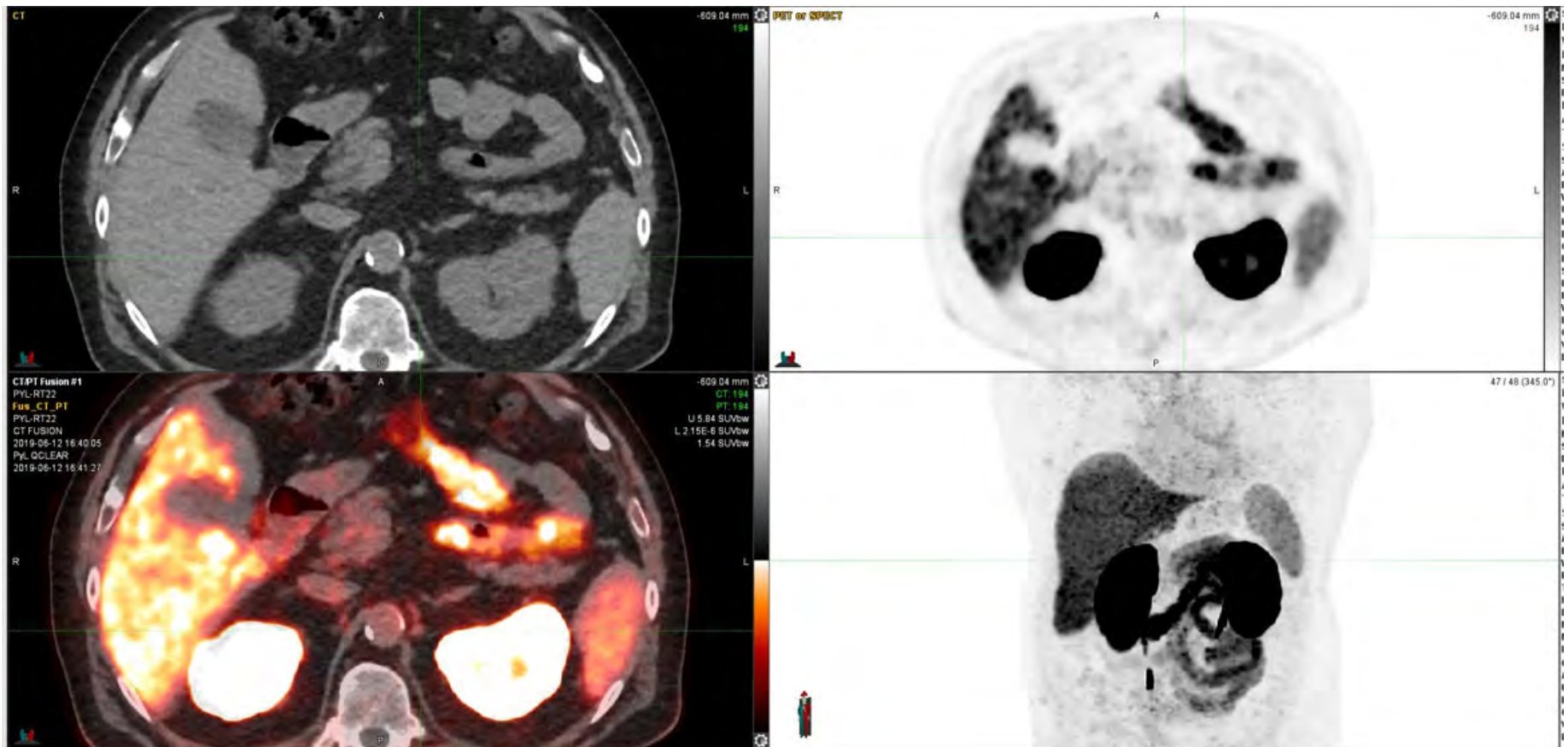
Adapted from Werner RA, et al. Recent updates on molecular imaging reporting and data systems (MI-RADS) for theranostic radiotracers-navigating pitfalls of SSTR- and PSMA-targeted PET/CT. J Clin Med. 2019 Jul 19;8(7)

*A definitive finding on CT means the presence of a real anatomical substrate on the CT

Image Interpretation Cases

Society of Nuclear Medicine and Molecular Imaging

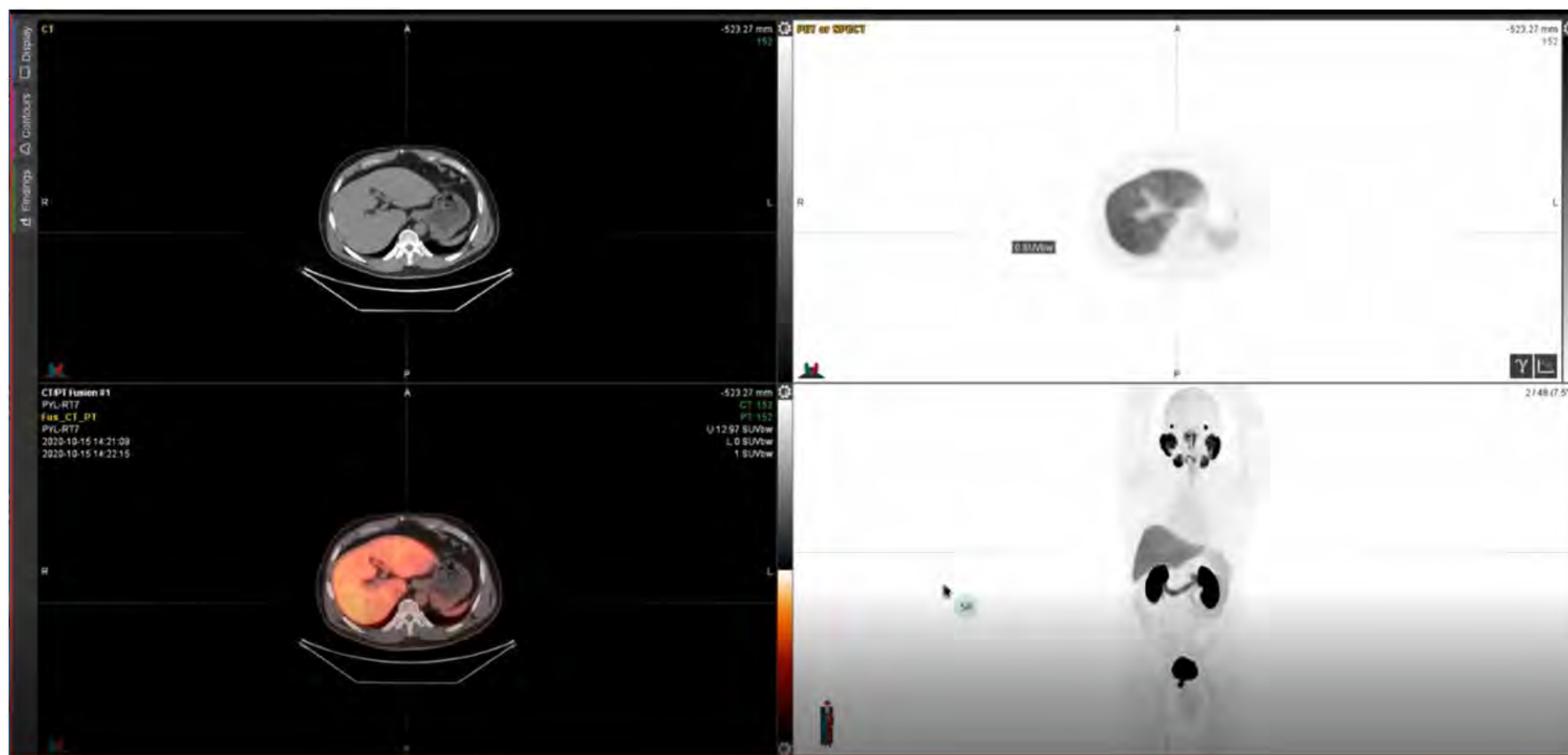
Case 1



[Click on image to play video](#)

Society of Nuclear Medicine and Molecular Imaging

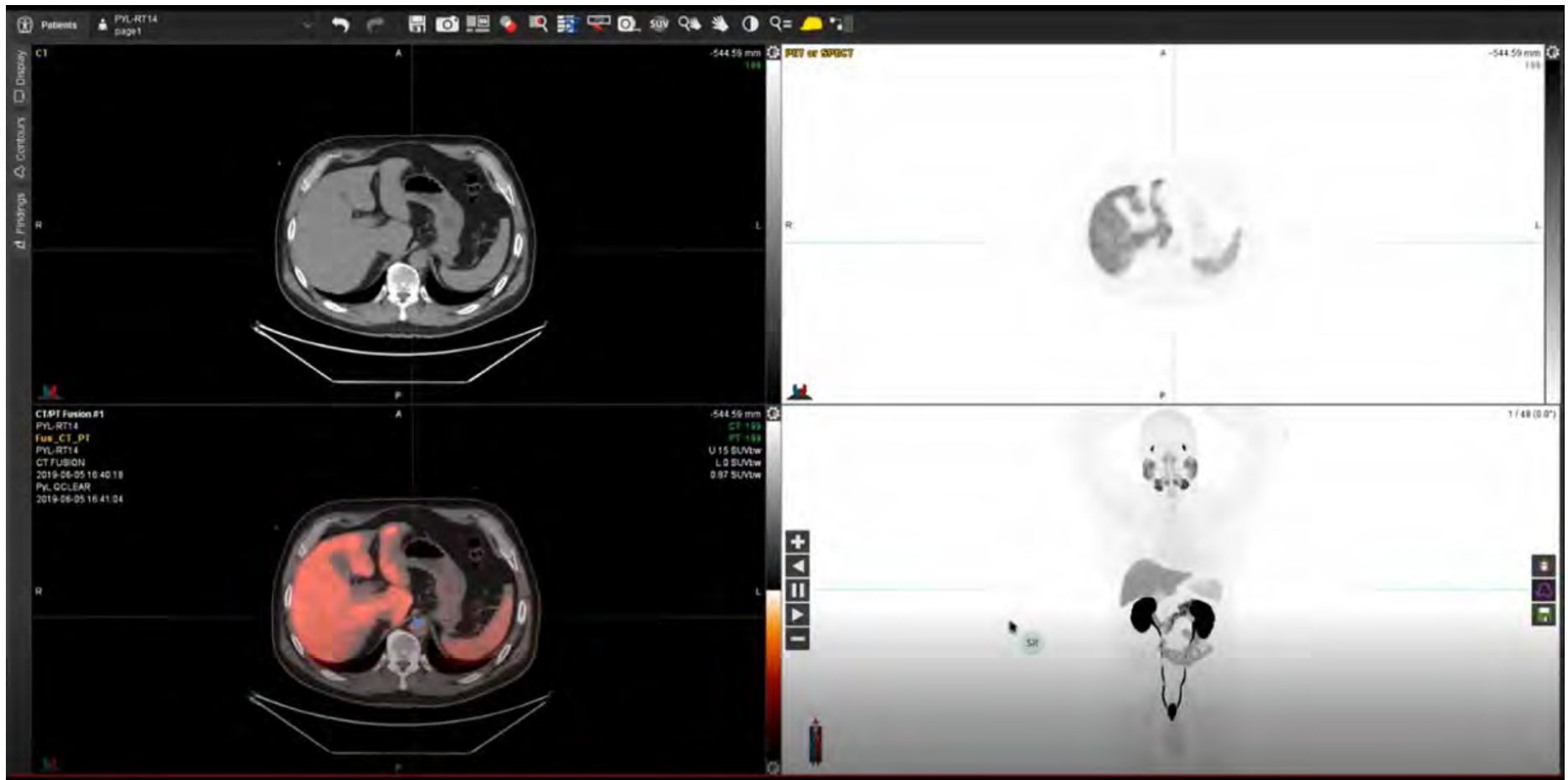
Case 2



[Click on image to play video](#)

Society of Nuclear Medicine and Molecular Imaging

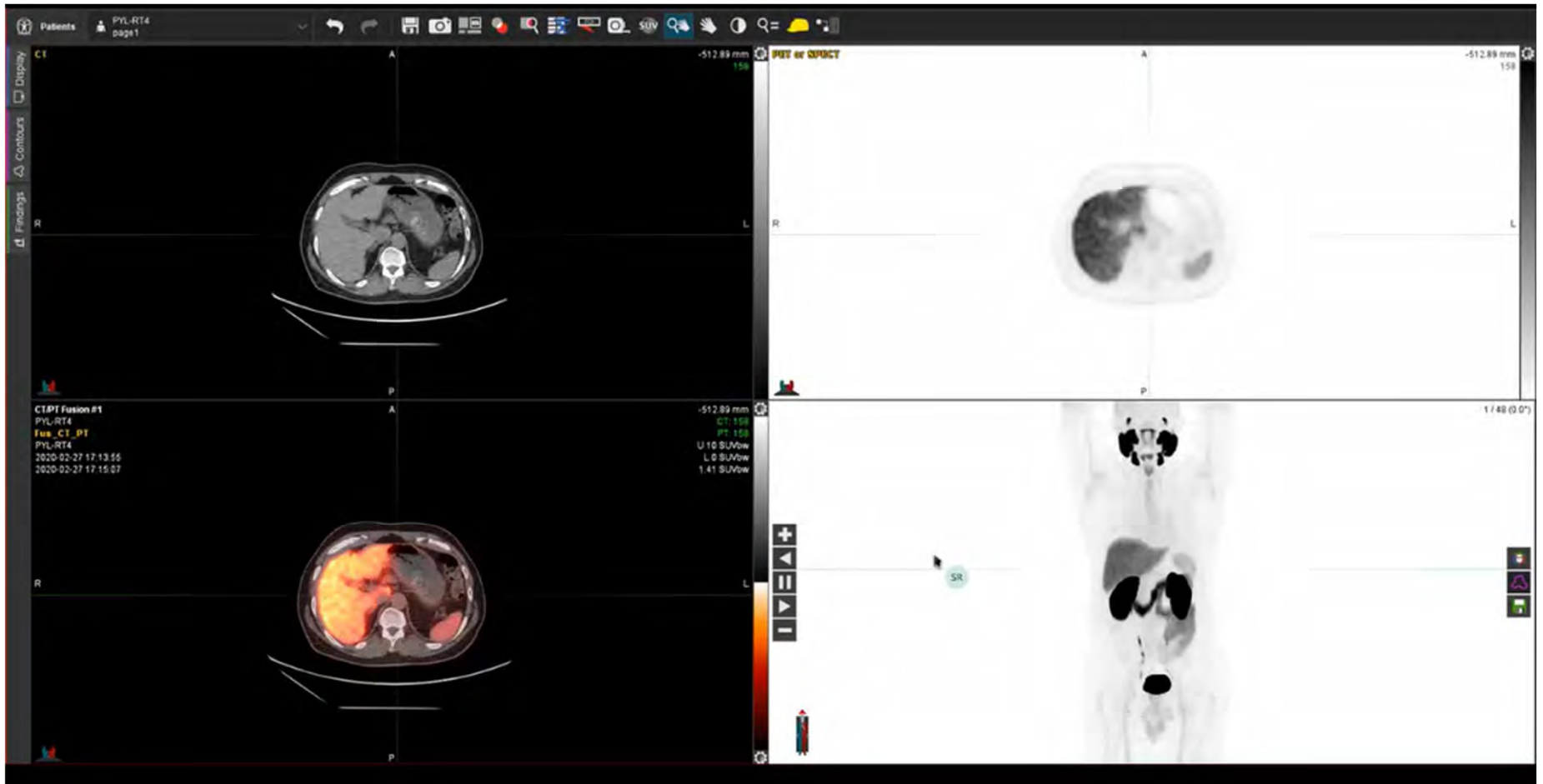
Case 3



[Click on image to play video](#)

Society of Nuclear Medicine and Molecular Imaging

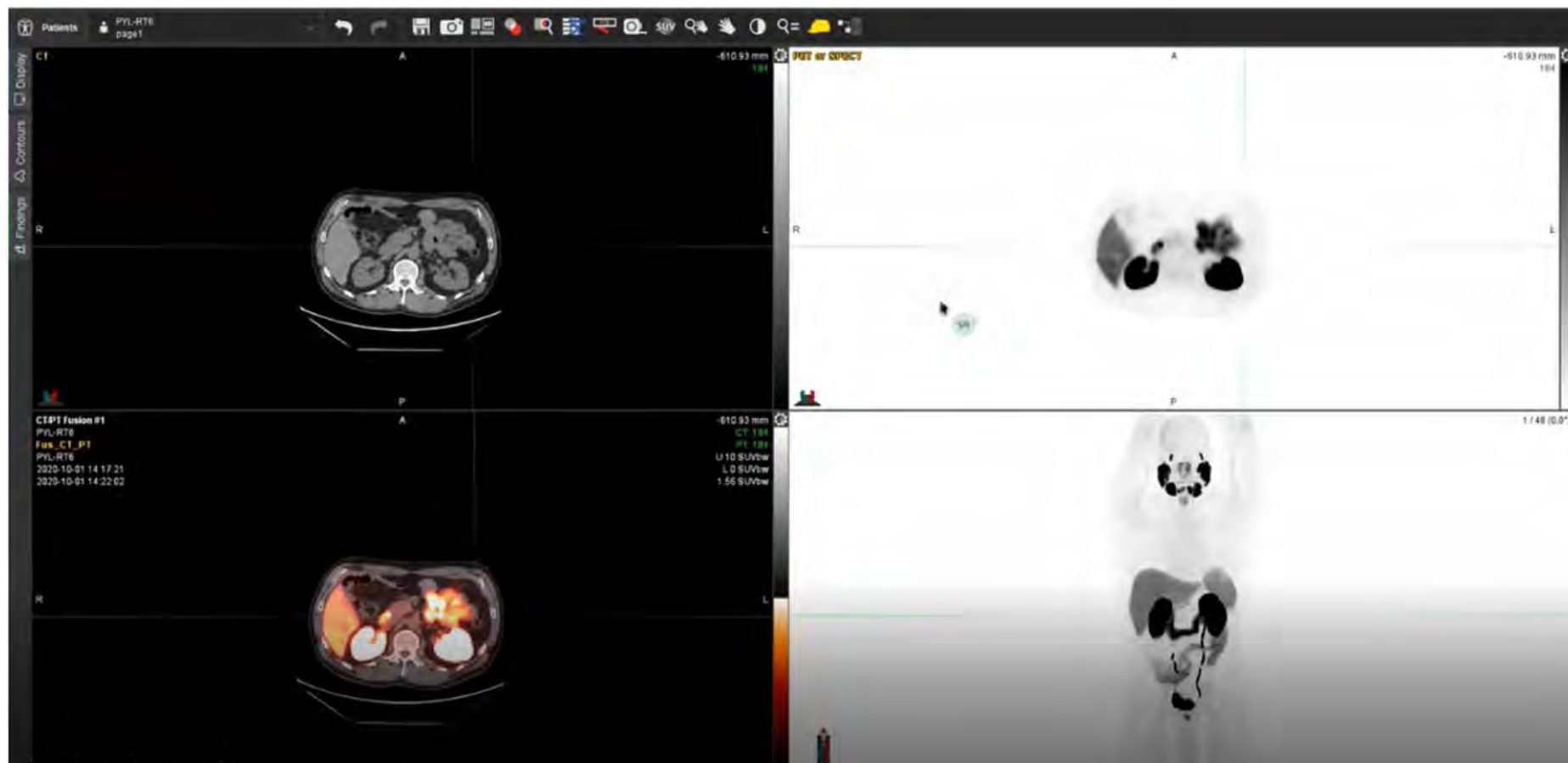
Case 4



[Click on image to play video](#)

Society of Nuclear Medicine and Molecular Imaging

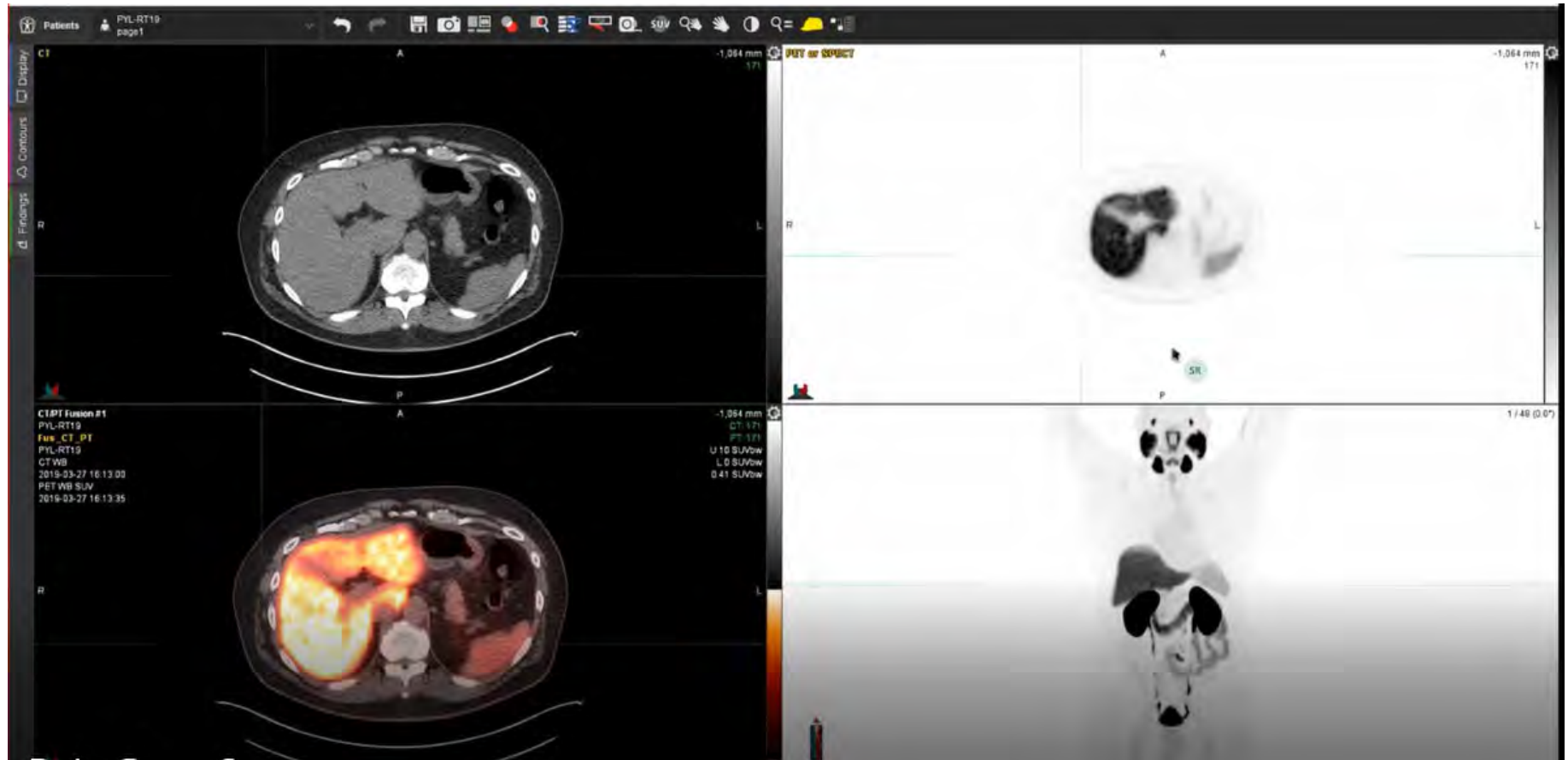
Case 5



[Click on image to play video](#)

Society of Nuclear Medicine and Molecular Imaging

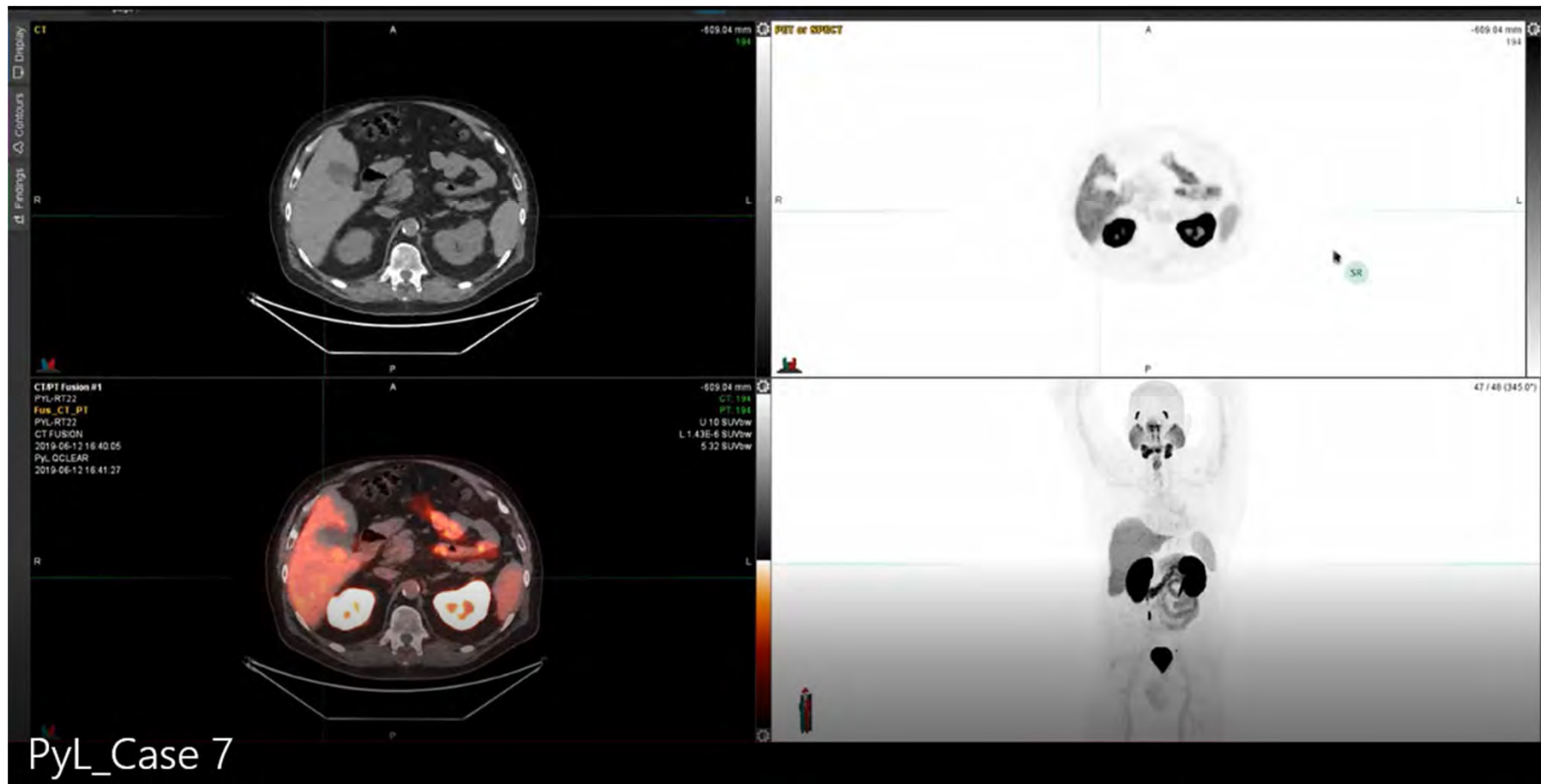
Case 6



[Click on image to play video](#)

Society of Nuclear Medicine and Molecular Imaging

Case 7



[Click on image to play video](#)

Society of Nuclear Medicine and Molecular Imaging

Case 8



[Click on image to play video](#)

Society of Nuclear Medicine and Molecular Imaging

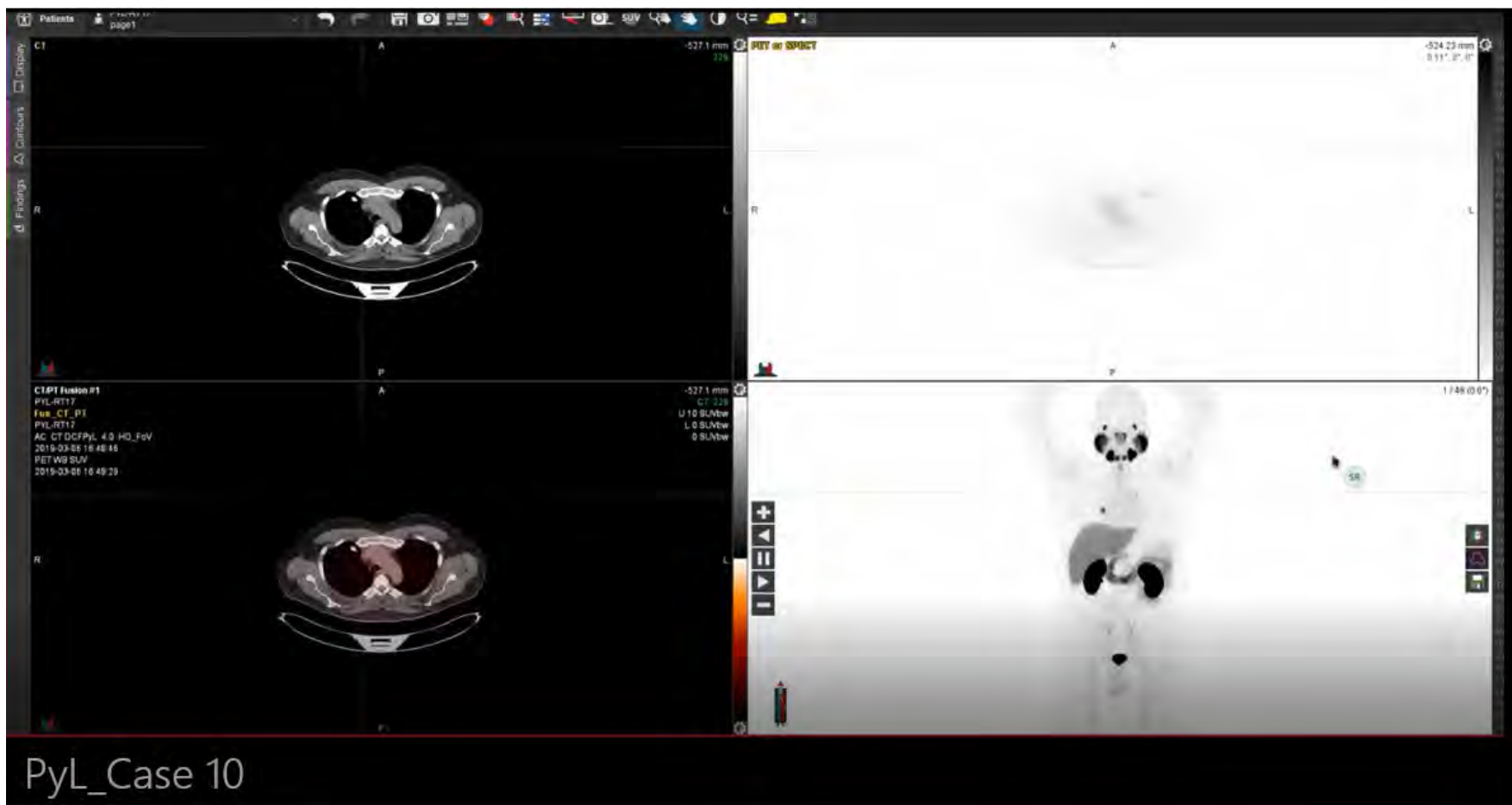
Case 9



[Click on image to play video](#)

Society of Nuclear Medicine and Molecular Imaging

Case 10



[Click on image to play video](#)
Society of Nuclear Medicine and Molecular Imaging

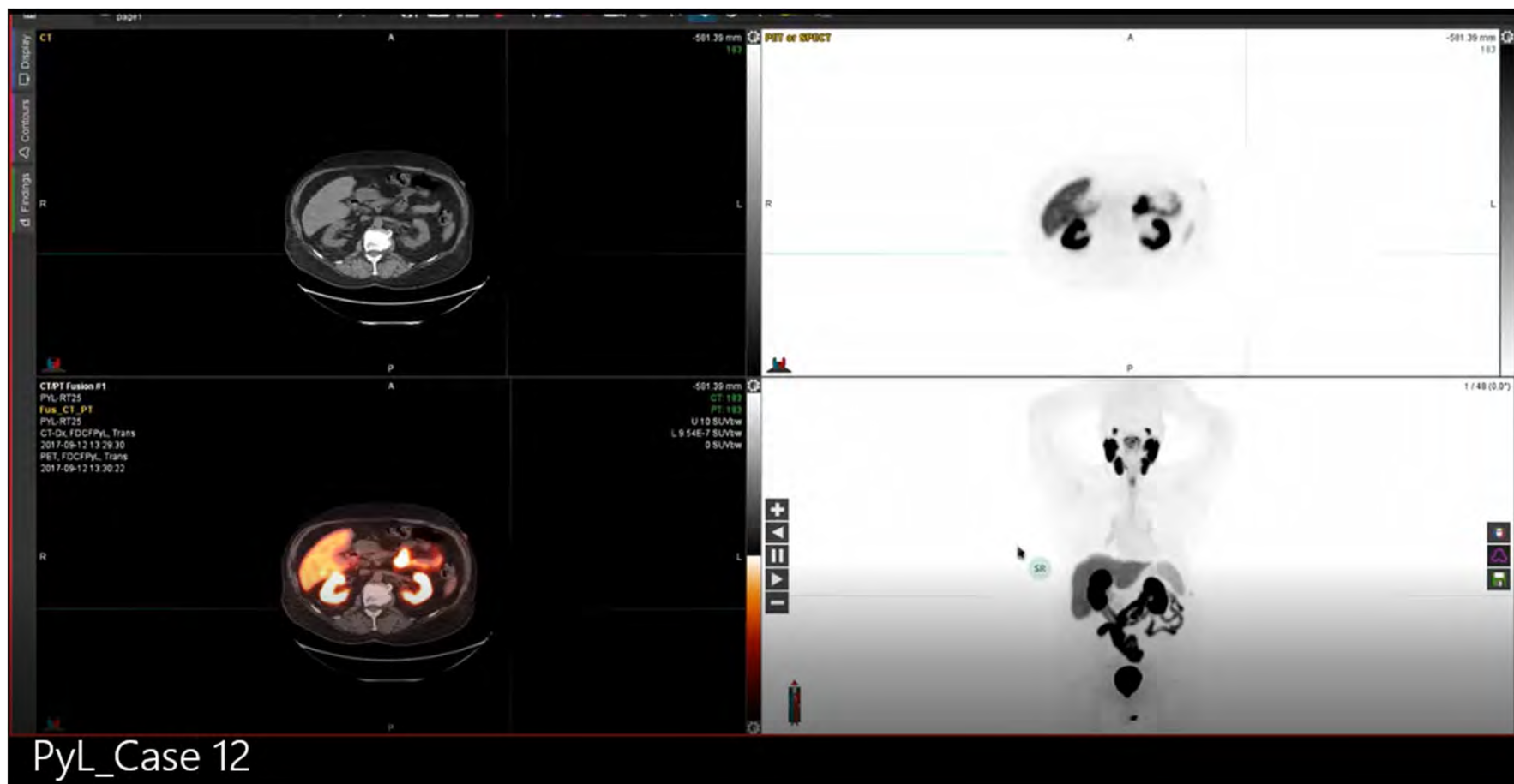
Case 11



[Click on image to play video](#)

Society of Nuclear Medicine and Molecular Imaging

Case 12



[Click on image to play video](#)

Society of Nuclear Medicine and Molecular Imaging

Case 13



[Click on image to play video](#)

Society of Nuclear Medicine and Molecular Imaging

Diolch Kiitos Sheun umesc. Kasih Mamnoon Todah
Shnorhakatutun Shokriya Ngiyabonga Dziękuje
Gamsahapnida Te'ekür Dekuju/Dekujeme Hvala
Dank Waad Kop Salamat Merci Gra or Xie
Dakujem Daw Dhanyavaadaalu Takk Dhanyavad Khopjai
Krap Tack Grazzi raibh Gracias Nandree Blagodariya
Gomapsupnida Fyrir Terima Enkosi Danke Euxaristo Kun
Shukriya Shokrun Spaas Mul Ači
Dankie Dhanyavaad Gra or Xie
Kruthagnathalu Faleminderit
Arigatou Dhonnobaad Asante
ederim Hain Dhan daa